Paxillus involutus-Facilitated Cd^{2+} Influx through Plasma Membrane Ca^{2+}-Permeable Channels Is Stimulated by H_2O_2 and H^+-ATPase in Ectomycorrhizal *Populus × canescens* under Cadmium Stress

Yuhong Zhang[1†], Gang Sa[1†], Yinan Zhang[1†], Zhimei Zhu[1], Shurong Deng[1], Jian Sun[2], Nianfei Li[1], Jing Li[3], Jun Yao[1], Nan Zhao[1], Rui Zhao[1], Xujun Ma[1], Andrea Polle[4] and Shaoliang Chen[1*]

[1] College of Biological Sciences and Technology, Beijing Forestry University, Beijing, China, [2] College of Life Science, Jiangsu Normal University, Xuzhou, China, [3] School of Computer Science and Technology, Henan Polytechnic University, Jiaozuo, China, [4] Büsgen-Institut, Forstbotanik und Baumphysiologie, Georg-August-Universität Göttingen, Göttingen, Germany

Using a Non-invasive Micro-test Technique, flux profiles of Cd^{2+}, Ca^{2+}, and H^+ were investigated in axenically grown cultures of two strains of *Paxillus involutus* (MAJ and NAU), ectomycorrhizae formed by these fungi with the woody Cd^{2+}-hyperaccumulator, *Populus × canescens,* and non-mycorrhizal (NM) roots. The influx of Cd^{2+} increased in fungal mycelia, NM and ectomycorrhizal (EM) roots upon a 40-min shock, after short-term (ST, 24 h), or long-term (LT, 7 days) exposure to a hydroponic environment of 50 μM $CdCl_2$. Cd^{2+} treatments (shock, ST, and LT) decreased Ca^{2+} influx in NM and EM roots but led to an enhanced influx of Ca^{2+} in axenically grown EM cultures of the two *P. involutus* isolates. The susceptibility of Cd^{2+} flux to typical Ca^{2+} channel blockers ($LaCl_3$, $GdCl_3$, verapamil, and TEA) in fungal mycelia and poplar roots indicated that the Cd^{2+} entry occurred mainly through Ca^{2+}-permeable channels in the plasma membrane (PM). Cd^{2+} treatment resulted in H_2O_2 production. H_2O_2 exposure accelerated the entry of Cd^{2+} and Ca^{2+} in NM and EM roots. Cd^{2+} further stimulated H^+ pumping activity benefiting NM and EM roots to maintain an acidic environment, which favored the entry of Cd^{2+} across the PM. A scavenger of reactive oxygen species, DMTU, and an inhibitor of PM H^+-ATPase, orthovanadate, decreased Ca^{2+} and Cd^{2+} influx in NM and EM roots, suggesting that the entry of Cd^{2+} through Ca^{2+}-permeable channels is stimulated by H_2O_2 and H^+ pumps. Compared to NM roots, EM roots exhibited higher Cd^{2+}-fluxes under shock, ST, and LT Cd^{2+} treatments. We conclude that ectomycorrhizal *P. × canescens* roots retained a pronounced H_2O_2 production and a high H^+-pumping activity, which activated PM Ca^{2+} channels and thus facilitated a high influx of Cd^{2+} under Cd^{2+} stress.

Keywords: ectomycorrhizal fungi, *Paxillus involutus*, MAJ, NAU, Cd^{2+}-hyperaccumulator, poplar, NMT

INTRODUCTION

The presence of highly toxic cadmium (Cd^{2+}) in the environment is a serious threat to human health as heavy metals can be enriched in plants and eventually enter the human body through the food chain (Nawrot et al., 2006; Kaplan et al., 2011). The genus *Populus* spp. is of particular interest for phytoremediation of Cd^{2+} pollution (Sell et al., 2005; Krpata et al., 2008, 2009; Kieffer et al., 2009; He et al., 2011, 2013, 2015; Ma Y. et al., 2014), due to its widespread distribution, rapid growth, and genotypic differences in response to ion-specific stress (Chen and Polle, 2010; Polle et al., 2013; Chen et al., 2014; Polle and Chen, 2015). *Populus tremula* (Kieffer et al., 2009) and *Populus × canescens* (He et al., 2011) have been recently identified as woody Cd^{2+}-hyperaccumulators. Cd^{2+} enrichment in these poplars (Kieffer et al., 2009; He et al., 2011; Ma Y. et al., 2014) exceed the threshold of 100 μg Cd^{2+} g^{-1} DW that has commonly been defined for hyperaccumulation (Milner and Kochian, 2008; Krämer, 2010). He et al. (2013) demonstrated that *P. × canescens* could detoxify Cd^{2+} by its sequestration in the bark.

In nature, poplar roots form symbioses with mycorrhizal fungi (Danielsen et al., 2012, 2013). For example, colonization of *P. × canescens* roots with the ectomycorrhizal fungus *Paxillus involutus* improves growth, primes for increased stress tolerance, increases nutrition, and regulates the ion balance under salt stress (Schützendübel and Polle, 2002; Gafur et al., 2004; Langenfeld-Heyser et al., 2007; Luo et al., 2009, 2011; Li J. et al., 2012; Ma X. et al., 2014). A notable finding was that *Paxillus involutus* ectomycorrhizas enhance both Cd^{2+} uptake and tolerance in *P. × canescens* (Ma Y. et al., 2014). Thus, ectomycorrhizal poplar plants offer a great potential for phytoremediation of Cd^{2+}-polluted soils (Sell et al., 2005; Krpata et al., 2008, 2009; Luo et al., 2014; Ma Y. et al., 2014).

Cd^{2+} is generally believed to enter plant cells through high affinity transporters responsible for the uptake of divalent cations (Cu^{2+}, Co^{2+}, Fe^{2+}, Ca^{2+}, Mn^{2+}, and Zn^{2+}; Liu et al., 1997; Clemens et al., 1998; Cohen et al., 1998; Hirschi et al., 2000; Thomine et al., 2000; Zhao et al., 2002; Cosio et al., 2004; Clemens, 2006; Roth et al., 2006). Cd^{2+} can even induce nutrient deficiencies by competing with the uptake of essential elements (Zhao et al., 2006; Papoyan et al., 2007; DalCorso et al., 2008; Gallego et al., 2012; Baliardini et al., 2015). On the other hand, elevated Ca^{2+} levels suppress Cd^{2+} uptake in different ecotypes of *Sedum alfredii* also supporting competition of Cd^{2+} uptake with nutrient cations (Lu et al., 2010). Transcript levels of the transporters involved in Cd^{2+} uptake and transport have been investigated in herbaceous and woody species (Kim et al., 2006; Plaza et al., 2007; Krämer, 2010; Migeon et al., 2010; Mendoza-Cózatl et al., 2011; Lin and Aarts, 2012). In poplar plants, a variety of heavy metal transporters, such as ZRT-IRT-like proteins (ZIP2, ZIP6.2), natural resistance associated macrophage proteins (NRAMP1.1, NRAMP1.3), ATP-binding cassette transporter C1 (ABCC1), heavy metal ATPase 4 (HMA4), ATP-binding cassette transporter in mitochondria (ATM3), have been suggested to play pivotal roles in Cd^{2+} transport and detoxification (Ma Y. et al., 2014; He et al., 2015). In addition

to these heavy metal transporters, ion channels in the plasma membrane (PM) that are permeable to Cd^{2+} contribute the Cd^{2+} uptake (Li et al., 2012a; Sun et al., 2013a,b; He et al., 2015). High external Cd^{2+} concentrations establish a large electrochemical gradient facilitating the rapid movement of Cd^{2+} ions through Cd^{2+}-permeable channels. Perfus-Barbeoch et al. (2002) suggested that Cd^{2+} enters root cells via plasma membrane (PM) Ca^{2+} channels.

Ca^{2+} channels in the PM have been characterized by electrophysiological measurements involving incorporation of plasma-membrane vesicles into planar lipid bilayers (PLB, White, 2000) and patch clamping (Perfus-Barbeoch et al., 2002). According to their electrophysiological properties, the channels can be divided into depolarisation-, hyperpolarisation-, elicitor-activated, and voltage-insensitive channels (Thuleau et al., 1998; White, 2000). These channels display different sensitivities to typical inhibitors of Ca^{2+} channels, such as La^{3+}, Gd^{3+}, TEA, and verapamil. Specifically, verapamil and TEA inhibit depolarisation-activated Ca^{2+} channels, such as the wheat root channel rca (Piñeros and Tester, 1997; White, 1998), and rye root voltage-dependent cation channel 2, VDCC2 (White, 1998). La^{3+} shares a high similarity to another trivalent cation, Gd^{3+}. Both cations are able to inhibit three distinct classes of Ca^{2+} channels, including depolarisation-activated Ca^{2+} channels, rca (Piñeros and Tester, 1997; White, 1998), hyperpolarisation-activated Ca^{2+} channels (HACCs) in onion bulb epidermis (Pickard and Ding, 1993), voltage-insensitive channels such as Arabidopsis root epidermal non-selective cation channels (NSCCs; Demidchik et al., 2002), and large-conductance elicitor-activated channel (LEAC) in parsley cell suspension (Zimmermann et al., 1997). Ca^{2+} channels in the PM are permeable to divalent (including Ca^{2+}, Mg^{2+}, Ba^{2+}, Sr^{2+}, Co^{2+}, Zn^{2+}, Mn^{2+}, Ni^{2+}, Cu^{2+}; Cosgrove and Hedrich, 1991; Ping et al., 1992; Pickard and Ding, 1993; Thuleau et al., 1994a,b; Gelli and Blumwald, 1997; Zimmermann et al., 1997; White, 1998; Grabov and Blatt, 1998, 1999) and monovalent cations (Na^+, K^+, Cs^+, Li^+, Rb^+; Cosgrove and Hedrich, 1991; Pickard and Ding, 1993; Zimmermann et al., 1997; Piñeros and Tester, 1997; White, 1998). In accordance with the suggestion that Cd^{2+} ions can be transported into cells through Ca^{2+} channels (Perfus-Barbeoch et al., 2002; Gallego et al., 2012; Li et al., 2012b) the permeability for Cd^{2+} through wheat VDCC2 was detected when the plasma membrane derived from root cells was incorporated into PLB (White, 1998). Using the whole-cell patch-clamp technique, Perfus-Barbeoch et al. (2002) confirmed that Cd^{2+} permeates through the PM Ca^{2+} channels in Arabidopsis guard cells. The Cd^{2+} influx was effectively blocked by Ca^{2+} channel blockers, e.g., $LaCl_3$ and verapamil in *Suaeda salsa* (Li et al., 2012a), *Populus euphratica* (Sun et al., 2013b), and *P. tremula × P. alba* (He et al., 2015), further indicating that Cd^{2+} ions penetrate into plant cells through Ca^{2+}-permeable channels.

It is possible that hydrogen peroxide (H_2O_2) stimulates the entry of Cd^{2+} through PM Ca^{2+} channels as the activity of these channels has been shown to be stimulated by H_2O_2. Pei et al. (2000) found that H_2O_2 activates the PM Ca^{2+} channels, leading to a subsequent rise of cytosolic Ca^{2+} in *Arabidopsis* guard cells. Demidchik et al. (2007) observed a transient increase

of Ca^{2+} influx in the root epidermis when exogenous H_2O_2 was applied to *Arabidopsis thaliana*. In NaCl-stressed *P. euphratica* cells, Ca^{2+} influx through Ca^{2+} channels was activated by H_2O_2 (Sun et al., 2010). Recently, H_2O_2 was shown to accelerate Cd^{2+} influx in *P. euphratica* cells, while the H_2O_2-stimulated Cd^{2+} influx was blocked by $LaCl_3$ (Sun et al., 2013b; Han et al., 2016). Moreover, the application of a H_2O_2 scavenger, catalase, lowered the Cd^{2+} influx across the PM in Cd^{2+}-stressed *P. euphratica* cells (Sun et al., 2013b). In Cd^{2+}-treated *P. euphratica* cells, hydrogen sulfide was found to reduce Cd^{2+} influx through down-regulation of H_2O_2-stimulated Cd^{2+} transport across the PM Ca^{2+} channels (Sun et al., 2013b). H_2O_2 is not only produced in Cd^{2+}-stressed poplar cells (Sun et al., 2013b; Han et al., 2016) and roots (Ma Y. et al., 2014; He et al., 2015), but is also massively enriched in *Populus × canescens–Paxillus involutus* ectomycorrhizal associations (Gafur et al., 2004; Langenfeld-Heyser et al., 2007). Thus, it can be speculated that the fungal-elicited H_2O_2 accelerates the entry of Cd^{2+} through PM Ca^{2+} channels. However, this hypothesis needs to be clarified by further electrophysiological investigations.

In addition to H_2O_2, the PM H^+-ATPase plays a crucial role in accelerating Cd^{2+} transport in poplar roots (Ma Y. et al., 2014; He et al., 2015). He et al. (2015) demonstrated that the net Cd^{2+} influx was pH-dependent in poplar roots and effectively blocked by inhibitors of H^+-pumps. Ma Y. et al. (2014) showed that the active PM H^+-ATPase-driven Cd^{2+} uptake is a major factor for increased Cd^{2+} accumulation in ectomycorrhizal (EM) poplar plants. They suggested that the EM-induced transcripts of *HA2.1* and *AHA10.1* genes, encoding PM H^+-ATPases in *P. × canescens*, may result in H^+-pump-stimulated Cd^{2+} enrichment (Ma Y. et al., 2014). In agreement with this suggestion transgenic poplars that were more Cd^{2+} tolerant by overexpression of γ-glutamylcysteine synthetase, showed upregulated transcript levels of *VHA1.1*, *HA2.1* and *AHA10.1* and a high Cd^{2+} uptake rate (He et al., 2015). The PM H^+-ATPases maintain a H^+ gradient across the membrane to promote active transport of essential elements across the PM (Beritognolo et al., 2007; Ma et al., 2010; Sun et al., 2010; Luo et al., 2013). Increased H^+-pumping activities have been well characterized in arbuscular mycorrhizal associations (Ramos et al., 2005; Rosewarne et al., 2007) and in ectomycorrhizal associations formed by *Paxillus involutus* (strains MAJ and NAU) with *Populus × canescens* (Li J. et al., 2012). We have previously shown that the upregulated H^+-pumping activities in *Paxillus involutus-Populus × canescens* symbiosis resulted in enhanced Ca^{2+} uptake and enrichment (Li J. et al., 2012). Demidchik et al. (2002) proposed that voltage modulation of the co-existing NSCC/HACC by PM H^+-ATPase would be a potent regulator for Ca^{2+} entry to the root cell cytoplasm. The high H^+-pumping activity leads to hyperpolarization of the PM and, thus, may increase Cd^{2+} influx through hyperpolarisation-activated Ca^{2+} channels. However, it is unknown whether the PM H^+-ATPases could stimulate the entry of Cd^{2+} through Ca^{2+}-permeable channels in ectomycorrhizal plants.

The two *P. involutus* strains, MAJ and NAU, form different colonization structures with *P. × canescens* roots (Gafur et al., 2004). Strain MAJ forms a typical hyphal mantle and Hartig

net with roots of *P. × canescens*, while NAU is unable to intrude between the host cells and forms only a hyphal mantle ensheathing the root tips (Gafur et al., 2004). The colonization of *P. × canescens* roots with the competent strain MAJ results in enriched Cd^{2+} levels under Cd^{2+} stress (Ma Y. et al., 2014). Whether the incompatible fungal isolate NAU also affects the Cd^{2+} entry into *P. × canescens* host plants needs to be clarified.

In this study, we used a non-invasive micro-test technique (NMT) to measure fluxes of Cd^{2+}, Ca^{2+} and H^+ in Cd^{2+}-stressed roots of non-mycorrhizal (NM) and ectomycorrhizal *P. × canescens* plants colonized with *Paxillus involutus* strains, MAJ and NAU. The aim was to elucidate whether the Cd^{2+} influx through Ca^{2+}-permeable channels is stimulated by H_2O_2 and H^+-ATPase in ectomycorrhizal roots since the ectomycorrhizas exhibit enhanced H_2O_2 production and upregulated H^+-pumping activity. NMT microelectrodes measure the ion fluxes on the surface of the tissues, which are either the plant root cells for the NM plants or the fungal hyphae forming the mantle structure ensheathing the roots. To discriminate between potentially different Cd^{2+} effects on fungus and plant roots, fluxes of Cd^{2+}, Ca^{2+} and H^+ were examined for pure fungal mycelia of the two *P. involutus* isolates, MAJ and NAU, in addition to flux recordings on NM and EM roots. Furthermore, flux profiles of Cd^{2+} and Ca^{2+} were recorded in *P. involutus*-inoculated roots after 7 days of co-culture. The aim was to determine whether flux profiles of mature EM associations resemble the pattern of those from host roots at early stages of fungal colonization when the host is known to activate transient defense responses in contrast to the mature ectomycorrhizal symbioses (Duplessis et al., 2005).

MATERIALS AND METHODS

Fungus and Plant Cultures for EM Colonization

The *Paxillus involutus* isolates MAJ and NAU, obtained from the Büsgen Institute: Institute of Forest Botany and Tree Physiology (Göttingen University, Germany), were grown on 2% modified Melin Norkrans (MMN) agar medium (g·L^{-1}): KH_2PO_4 0.5, $(NH_4)_2SO_4$ 0.25, $MgSO_4·7H_2O$ 0.15, $CaCl_2·2H_2O$ 0.05, NaCl 0.025, $FeCl_3·6H_2O$ 0.01, thiamine HCl 0.0001, glucose 10, malt extract 3, pH 5.2 (Gafur et al., 2004; Li J. et al., 2012). Prior to the colonization, the fungi were pre-grown on the agar culture medium for 1 week in petri dishes (diameter 90 mm) and kept in darkness at 23°C.

Plantlets of *Populus × canescens* (a hybrid of *Populus tremula × Populus alba*) were propagated by micropropagation as described by Leple et al. (1992). Regenerated *P. × canescens* plants were grown for 3–4 weeks on Murashige and Skoog (MS) medium (Murashige and Skoog, 1962). Uniform plants with sufficient roots were used for ectomycorrhization. The colonization of *P. × canescens* with *Paxillus involutus* strains MAJ and NAU was followed the procedures described by Gafur et al. (2004). In brief, rooted plantlets from sterile culture were placed on the MMN agar medium in the presence or absence of EM mycelium. After fungal inoculation, the petri dishes were

sealed with Parafilm and covered with aluminum foil to keep the roots in darkness. During the period of incubation, the temperature in the climate chamber was maintained at 23°C with a light period of 16 h (6:00 AM–22:00 PM). Photosynthetic active radiation (PAR) of 200 μmol m^{-2} s^{-1} was supplied by cool white fluorescent lamps. After 1 month of inoculation, EM and NM root tips for anatomical investigations were embedded, stained, and photographed as described previously (Gafur et al., 2004). EM and NM plants with similar height and growth performance were used for CdCl$_2$ treatment.

Liquid Culture of Fungi

Liquid culture of *P. involutus* was grown as previously described (Ott et al., 2002; Langenfeld-Heyser et al., 2007; Li J. et al., 2012). In brief, mycelium from the agar plate was homogenized, transferred into 100 mL of liquid medium (pH 4.8) in flasks, and incubated on a rotary shaker in darkness (150 rpm, 23°C). *P. involutus* in submerged culture grew in the form of compact spherical masses of mycelium (pellets). For Cd^{2+} shock treatment, sterile filtered CdCl$_2$ solutions were added to achieve final concentrations of 50 μM. After ST (24 h) or LT (7 days) treatment, axenic cultures of MAJ and NAU were used for steady flux measurements of Cd^{2+}, H$^+$, and Ca^{2+}.

Cadmium Treatment

Ectomycorrhizal and non-mycorrhizal plants were carefully removed from MMN agar medium. Rooted plantlets were cultivated in individual pots containing hydroponic MS nutrient solution (MS medium without agar and sucrose) (Murashige and Skoog, 1962). Plants were covered with plastic bags to reduce the rapid water loss in a growth room. NM and EM plantlets were subjected to 50 μM CdCl$_2$ for a short-term (ST) exposure, 24 h or a long-term (LT) exposure for 7 days. The required amount of CdCl$_2$ was added to the MS nutrient solution. Control plants were treated in the same manner without the addition of CdCl$_2$. The plants were maintained at 23°C with a light period of 16 h (6:00 AM–22:00 PM) and PAR was 200 μmol m^{-2} s^{-1}. Plants were continuously aerated by passing air to hydroponic MS nutrient solution, which was regularly renewed. Steady fluxes of Cd^{2+}, Ca^{2+} and H$^+$ in NM and EM roots were examined after 24 h and 7 days of CdCl$_2$ treatment. In addition, ST-induced alterations of Cd^{2+} and Ca^{2+} fluxes were also examined in non-inoculated and *P. involutus*-inoculated roots after 7 days of co-culture.

Measurements of Net Cd^{2+}, Ca^{2+}, and H$^+$ Fluxes

Preparations of Ion-Selective Microelectrodes

Non-invasive Micro-test Technique (NMT-YG-100, Younger USA LLC, Amherst, MA01002, USA) with ASET 2.0 (Sciencewares, Falmouth, MA 02540, USA) and iFluxes 1.0 Software (Younger USA, LLC, Amherst, MA 01002, USA) was used to monitor fluxes of Cd^{2+}, Ca^{2+} and H$^+$ in EM and NM roots (Sun et al., 2009a,b; Sun et al., 2013a,b; Ma X. et al., 2014). Ion-selective electrodes were prepared as described in Sun et al. (2009a, 2013a) and Ma X. et al. (2014). Briefly, pre-pulled and silanized glass micropipettes (diameter 4–5 μm, XY-DJ-01;

Xuyue (Beijing) Science and Technology Co. Ltd., Beijing, China) were back-filled with backfilling solution [Cd^{2+} microelectrodes: 10 mM Cd(NO$_3$)$_2$ and 0.1 mM KCl; Ca^{2+} microelectrodes: 100 mM CaCl$_2$; H$^+$ microelectrodes: 40 mM KH$_2$PO$_4$ and 15 mM NaCl, pH 7.0] to a length of 1.0 cm from the tip. Then the micropipettes were front-filled with 15 μm columns of selective liquid ion exchange cocktails (LIXs) (Cd: Fluka 20909, Sigma–Aldrich, St Louis, MO, USA; Ca: Fluka 21048; H: Fluka 95293 Fluka Chemie GmbH, Buchs, Switzerland). An Ag/AgCl wire electrode holder (XYEH01-1; Xuyue Sci. and Tech. Co., Ltd.) was inserted in the back of the electrode to create an electrical contact with the electrolyte solution. DRIREF-2 (World Precision Instruments, Inc., Sarasota, FL, USA) was used as the reference electrode (CMC-4). Prior to the measurements, ion-selective microelectrodes for the target ions were calibrated by the following standard solution:

(1) Cd^{2+}: 0.01, 0.05, 0.1 mM (Cd^{2+} concentration was 0.05 mM in the measuring solution);
(2) Ca^{2+}: 0.1, 0.5, 1.0 mM (Ca^{2+} was 0.2 mM in the measuring buffer);
(3) H$^+$: pH 4.2, 5.2, 6.2 (pH of the measuring solution was adjusted to 5.2 with KOH and HCl for root samples).

Electrodes were used when the Nernstian slopes in ranges of 29 ± 3 mV/decade (Cd^{2+}, Ca^{2+}) and 58 ± 5 mV/decade (H$^+$). The flux rate was calculated on the basis of Fick's law of diffusion:

$$J = -D\,(dc/dx),$$

where J is the ion flux in the x direction, D is the ion diffusion coefficient in a particular medium, dc represents the ion concentration difference, dx is the microelectrode movement between two positions, and dc/dx represents the ion concentration gradient. As part of the NMT system, ASET software [Science Wares (East Falmouth, MA, USA) and Applicable Electronics], was used for data and image acquisition, preliminary processing, control of three-dimensional electrode positioner and stepper-motor-controlled fine focus of the microscope stage.

Experimental Protocols for Steady-State Flux Measurements

Cd^{2+}, Ca^{2+}, and H$^+$ fluxes were non-invasively measured by moving the ion-selective microelectrode between two positions close to the materials in a preset excursion (30 μm for excised roots and fungal mycelia) at a programmable frequency in the range of 0.3–0.5 Hz. *P. involutus* mycelia, EM and NM roots from the ST and LT CdCl$_2$ treatments were rinsed with re-distilled water for 2–3 times, and then incubated in the basic measuring solution to equilibrate for 25 min. The concentration gradients of Cd^{2+}, Ca^{2+}, and H$^+$ were measured as previously described (Li J. et al., 2012; Lu et al., 2013; Sun et al., 2013a,b).

(1) Cd^{2+} measuring solutions: 0.1 mM KCl, 0.1 mM MgCl$_2$, 0.05 mM CaCl$_2$ and 0.05 mM CdCl$_2$, pH was adjusted to 5.2 with KOH and HCl;

(2) Ca^{2+} measuring solutions: 0.1 mM NaCl, 0.1 mM $MgCl_2$, 0.1 mM KCl, and 0.2 mM $CaCl_2$, pH was adjusted to 5.2 with KOH and HCl;

(3) H^+ measuring solutions: 0.1 mM NaCl, 0.1 mM $MgCl_2$, 0.1 mM $CaCl_2$ and 0.5 mM KCl, pH 5.2 was adjusted with KOH and HCl.

The steady fluxes of roots were then recorded 100 μm from the apex and conducted along the root axis until 2300 μm at intervals of 200–300 μm. The fluxes of each measuring point in apical regions were continuously recorded for 6–8 min. For *P. involutus* mycelia, Cd^{2+}, Ca^{2+}, and H^+ fluxes were measured around the surface of pelleted hyphae over a recording period of 30 min.

Transient Flux Recording

Paxillus involutus fungal mycelia and roots sampled from EM and NM plants were immobilized in the measuring solutions of Cd^{2+} (0.1 mM KCl, 0.1 mM $MgCl_2$, 0.05 mM $CaCl_2$, pH 5.2); Ca^{2+} (0.1 mM NaCl, 0.1 mM $MgCl_2$, 0.1 mM KCl, and 0.2 mM $CaCl_2$, pH 5.2) and H^+ (0.1 mM NaCl, 0.1 mM $MgCl_2$, 0.1 mM $CaCl_2$ and 0.5 mM KCl, pH 5.2) for 25 min equilibration. Then the steady-state fluxes in fungal mycelia and the root apical region (100 μm from the root apex) were continuously recorded for 5 min prior to the $CdCl_2$ shock. $CdCl_2$ stock (100 μM) was slowly added to the measuring solution using a pipette until the final Cd^{2+} concentration reached 50 μM. Afterward, transient kinetics of Cd^{2+}, Ca^{2+}, and H^+ were restarted and continued for 40 min. The data measured during the first 1–2 min was discarded, due to the effects of the diffusing stock solution. The high flux of Cd^{2+}, Ca^{2+}, and H^+ during the following 2 min was defined as peaking values.

Effects of H_2O_2 on $CdCl_2$-altered transient kinetics of Cd^{2+} and Ca^{2+} were also examined in NM and EM roots. Following the $CdCl_2$ shock (50 μM) as described above, H_2O_2 (1.0 mM) was introduced to the measuring solution and transient kinetics of Cd^{2+} and Ca^{2+} were recorded for 20 min.

Fungal mycelia were exposed to 50 μM $CdCl_2$ to induce a shock. Cd^{2+}, Ca^{2+}, and H^+ fluxes were monitored over a continuous recording period of 40 min. For transient flux kinetics, the data measured during the first 1–2 min were discarded due to the diffusion effects of stock addition.

Effects of Ca^{2+} on Sensitivity of Cd^{2+} Electrodes

To determine whether Ca^{2+} ions compete with Cd^{2+} to penetrate across PM Ca^{2+}-permeable channels, the effects of additional Ca^{2+} ions on Cd^{2+} electrodes was examined. Cd^{2+} calibrating solutions were added with 0, 0.01, 0.025, 0.05, 0.1, 0.2, 0.5, 1.0, or 2.0 mM Ca^{2+}. Then Cd^{2+} microelectrodes were calibrated in Ca^{2+}-supplemented solutions as described above. Moreover, the Nernst slope and intercept of the Cd^{2+} electrodes were calibrated in the measuring solution containing 0.1 mM KCl, 0.1 mM $MgCl_2$, and 0.05 mM $CaCl_2$.

Flux Oscillations

Oscillations in membrane-transport activity are ubiquitous in plant response to salinity, temperature, osmotic, hypoxia, and pH

stresses (Shabala et al., 2006). In our study, rhythmic (ultradian) flux oscillations in NM and EM *P. × canescens* roots were not noticeable as that observed in herbaceous species (Shabala et al., 1997, 2003, 2006; Shabala and Knowles, 2002). This finding is presumably due to a lower growth rate of woody roots compared with crop species (Li J. et al., 2012). The flux oscillations of the measured ions, e.g., H^+, Ca^{2+}, and Cd^{2+}, were more like fluctuations as previously reported in poplar roots (e.g., Na^+, K^+, H^+, and Ca^{2+}; Li J. et al., 2012). In this study, H^+, Ca^{2+}, and Cd^{2+} fluxes were recorded for 6–8 min at each point, which is long enough to cover oscillatory periods of measured ions.

Inhibitor and Stimulator Treatment

In this study, the effects of Ca^{2+}, pH, H_2O_2, and PM transporter and channel inhibitors on Cd^{2+}-altered ion flux profiles were examined in fungal mycelia and roots (NM and EM). Briefly,

Series 1: Ca^{2+} channel inhibitors. NM and EM roots were pre-treated with or without $LaCl_3$ (5 mM; Sun et al., 2010; Li et al., 2012b), $GdCl_3$ (500 μM, Demidchik et al., 2007, 2009; Sun et al., 2012), TEA (50 μM, White, 1998; Li J. et al., 2012), or verapamil (20 μM, Li et al., 2012a; He et al., 2015) for 24 h in the presence and absence of 50 μM $CdCl_2$. Fungal mycelia of the two *P. involutus* isolates, MAJ and NAU, were subjected to 0 or 5 mM $LaCl_3$ treatment for 24 h supplemented with or without 50 μM $CdCl_2$.

Series 2: Ca^{2+}. After being subjected to Cd^{2+} stress ($CdCl_2$, 50 μM) for 24 h, NM and EM roots were then exposed to 25, 50, or 100 μM $CaCl_2$ for flux recordings in the presence of $CdCl_2$.

Cd^{2+} and Ca^{2+} fluxes in Series 1 and 2 were measured along root axes, 100–2,300 μm from the apex, at intervals of 200–300 μm. In *P. involutus* mycelia, Cd^{2+} and Ca^{2+} fluxes were continuously measured around the surface of pelleted hyphae over a recording period of 30 min.

Series 3: Hydrogen peroxide. NM and EM roots were sampled and immobilized in Cd^{2+} or Ca^{2+} measuring solutions for transient flux recordings in the apical region (100 μm from the root apex). The steady-state fluxes were continuously recorded for 10–20 min prior to the $CdCl_2$ shock. $CdCl_2$ stock (100 μM) was slowly added to the measuring solution until the final Cd^{2+} concentration reached 50 μM and transient kinetics of Cd^{2+} and Ca^{2+} were continuously for 20–30 min. Afterward, H_2O_2 (1.0 mM) was slowly added to the measuring solution and transient kinetics of Cd^{2+} and Ca^{2+} were restarted and continued for 20 min.

Series 4: ROS scavenger. NM and EM roots were pre-treated with or without 1, 3-Dimethyl-2-thiourea (DMTU, 5 mM, Chung et al., 2008; Sun et al., 2010) for 24 h in the presence and absence of 50 μM $CdCl_2$. Then Cd^{2+} and Ca^{2+} fluxes were measured along root axes, 100–2,300 μm from the apex, at intervals of 200–300 μm.

Series 5: External pH. NM and EM roots were pre-treated with 50 μM $CdCl_2$ for 24 h prior to flux measurements. Cd^{2+} and Ca^{2+} fluxes along root axes (100–2,300 μm from the apex) were recorded in Cd^{2+} or Ca^{2+} measuring solutions at pH 5.2, 6.2, or 7.2, respectively.

Series 6: PM H^+-ATPase inhibitor. NM and EM roots were pre-treated with or without sodium orthovanadate (500 μM, Sun

et al., 2010; Lu et al., 2013) for 24 h in the presence and absence of 50 μM $CdCl_2$. Then H^+, Cd^{2+}, and Ca^{2+} fluxes were measured along root axes, 100–2,300 μm from the apex, at intervals of 200–300 μm. *P. involutus* isolates, MAJ and NAU, were exposed to 0 or 500 μM sodium orthovanadate for 24 h prior to a 30-min of continuous recording of H^+ flux.

Measurements of Net H_2O_2 Fluxes

An H_2O_2-sensitive microelectrode [tip diameter 2–3 μm, XY-DJ-502, Xuyue (Beijing) Science and Technology Co. Ltd., Beijing, China] was used to monitor H_2O_2 fluxes in EM and NM roots. H_2O_2 microelectrodes were prepared according to the method described by Twig et al. (2001). Before the measurement, H_2O_2 microelectrode was polarized at +0.60 V against an Ag/AgCl reference electrode. Thereafter, the microelectrodes were calibrated by the standard solution: 0.01, 0.1 and 1 mM H_2O_2. Roots sampled from control and $CdCl_2$ (50 μM,30 min)-treated EM and NM plants were immobilized in the measuring solution (0.1 mM NaCl, 0.1 mM $MgCl_2$, 0.1 mM $CaCl_2$ and 0.5 mM KCl, pH was adjusted to 5.2 with KOH and HCl) and equilibrated for 25 min. The fluxes were recorded 100 μm from the apex and conducted along the root axis until 2300 μm, at intervals of 200–300 μm, and then calculated.

Data Analysis

Ionic fluxes were calculated using the program JCal V3.2.1, a free MS Excel spreadsheet, which was developed by the Yue Xu[1]. The experimental data were subjected to SPSS (SPSS Statistics 17.0, 2008) for statistical tests and analyses. Unless otherwise stated, $P < 0.05$ was considered as significant.

RESULTS

Cd^{2+}-Altered Ion Flux Profiles in *Paxillus involutus,* and Roots of NM and EM Poplar

Cd^{2+} Fluxes

We recorded transient Cd^{2+} kinetics upon Cd^{2+} shock at the root apex (100 μm from the root tip; **Figure 1A**), where a vigorous ion flux (e.g., Na^+, K^+, Ca^{2+}, Cd^{2+}, Cl^-) is usually observed in woody and herbaceous plants (Sun et al., 2009a,b; Li J. et al., 2012; Lu et al., 2013; Han et al., 2014). The addition of $CdCl_2$ (50 μM) caused an immediate Cd^{2+} influx in both EM and NM roots which declined with increasing duration of Cd^{2+} exposure (40 min; **Figure 1A**). The peak and mean flux rate of Cd^{2+} in EM roots with MAJ were significantly (13.5 and 38.8%) higher than in NM roots or NAU-colonized roots (**Figure 1A**). Similar to the Cd^{2+} kinetics in EM roots, an instantaneous increase in the Cd^{2+} influx was detected in pure *P. involutus* mycelia after $CdCl_2$ exposure (50 μM; **Figure 1A**). However, the fungal Cd^{2+} influx remained constant over the recording period (40 min; **Figure 1A**) with significantly higher flux rates in MAJ (75.4 pmol cm^{-2} s^{-1}) than in NAU (25.9 pmol cm^{-2} s^{-1}).

After ST (24 h) or LT (7 days) exposure to 50 μM $CdCl_2$ in hydroponic conditions, steady-state Cd^{2+} flux was recorded along root axis (100–2,300 μm from the apex) at intervals of 200–300 μm (**Figure 2**). In NM roots, ST and LT stress caused a net Cd^{2+} influx with an overall mean of 28.9 pmol cm^{-2} s^{-1} along the whole measured distance; LT treatment resulted in a higher flux rate at the region 100–1,000 μm from the apex than at more distant root positions (**Figure 2**). A similar trend was observed in the Cd^{2+}-stressed EM roots, though mean Cd^{2+} fluxes in MAJ- and NAU-ectomycorrhizal roots were 43.1 and 32.0% higher than those of the NM roots under ST and LT stress (**Figure 2**). The mycelia of the two *P. involutus* strains, MAJ and NAU, exhibited a stable Cd^{2+} influx under ST and LT stress, although the $CdCl_2$-induced Cd^{2+} influx was typically higher under LT conditions, 68.9 pmol cm^{-2} s^{-1}, compared with ST treatment, 27.1 pmol cm^{-2} s^{-1} (**Figure 2**). Cd^{2+}-induced alterations of Cd^{2+} flux were also examined in non-inoculated and *P. involutus*-inoculated roots after 7 days of co-culture. NAU- and MAJ-colonized roots showed larger flux rates than non-inoculated roots after ST Cd^{2+} stress (Supplementary Figure S1A).

Our data show that *P. involutus* mycelia and EM roots both exhibited an enhanced Cd^{2+} uptake upon Cd^{2+} shock, ST, or LT treatment (**Figures 1A** and **2**). Unexpectedly, the Cd^{2+} influx in EM roots did not show a high correlation to the flux rate of Cd^{2+} in fungal hyphae under various treatments (shock, ST, or LT, Supplementary Figure S2). However, a relatively high correlation between EM and NM roots was observed especially in response to Cd^{2+} shock (Supplementary Figure S2). This result supports that in the ectomycorrhizal symbioses the continuous Cd^{2+} entry detected by NMT microelectrodes depends on the uptake capacity of inner root cells and that in the plant–fungal interaction divergent regulation of fungal Cd^{2+} transport compared with pure mycelium must take place.

Ca^{2+} Fluxes

In the absence of Cd^{2+} stress, poplar roots exhibited a net Ca^{2+} influx, with a greater flux rate in MAJ- and NAU-ectomycorrhizal roots, 26.9 pmol cm^{-2} s^{-1}, than in NM roots, 9.6 pmol cm^{-2} s^{-1} (**Figure 1B**). Similarly, the mycelia of the two strains exhibited a stable and steady influx of Ca^{2+} (162.3 pmol cm^{-2} s^{-1}), which is ca. 6.0-fold higher than that detected in EM roots (**Figure 1B**). $CdCl_2$ shock (50 μM) caused a transient Ca^{2+} efflux in NM and EM roots with maximum values ranging from 10.9 to 14.8 pmol cm^{-2} s^{-1} (**Figure 1B**). Thereafter, the direction shifted toward an influx and the mean flux over the recording period then declined in EM roots, or displayed a net efflux in NM roots (**Figure 1B**). In contrast to NM and EM roots, Cd^{2+} addition markedly increased the Ca^{2+} influx in the hyphae of pure mycelium, typically with higher flux rates in strain NAU than in MAJ in the first 20 min of Cd^{2+} application (**Figure 1B**). Under ST and LT treatment, Cd^{2+} stress caused a marked decline of Ca^{2+} influx along the root axis (**Figure 3**). MAJ- and NAU-ectomycorrhizal roots maintained 40.5 and 20.6% higher Ca^{2+} fluxes than NM roots under ST and LT stress (**Figure 3**). In the hyphae of the two fungal strains, the Ca^{2+} influx was enhanced by ST and LT treatments (**Figure 3**), similar to the shock treatment (**Figure 1B**). We observed that the

FIGURE 1 | Effects of CdCl$_2$ on transient kinetics of Cd^{2+}, Ca^{2+}, and H$^+$ in *Populus* × *canescens* roots and *Paxillus involutus* strains MAJ and NAU. Cd^{2+} **(A)**, Ca^{2+} **(B)**, and H$^+$ **(C)** kinetics were recorded before and after the required amount of 50 μM CdCl$_2$ was introduced into the measuring chamber. Prior to the CdCl$_2$ shock, steady-state fluxes of Cd^{2+}, Ca^{2+}, and H$^+$ in ectomycorrhizal (MAJ and NAU) and non-mycorrhizal (NM) *P.* × *canescens* roots (measuring site was ca. 100 μm from the root tip) and *P. involutus* isolates were monitored for approximately 5 min. Transient kinetics of Cd^{2+}, Ca^{2+}, and H$^+$ were recorded after the required amount of 50 μM CdCl$_2$ was introduced into the measuring solution. Inserted sections show the peaking and/or mean values of Cd^{2+}, Ca^{2+}, and H$^+$ flux before (−Cd) and after (+Cd) the addition of CdCl$_2$. Columns represent the mean of four to five individual plants or axenic EM cultures (pelleted hyphae), and bars represent the standard error of the mean. Different letters, a, b, c, d, e, and f, indicate significant difference at $P < 0.05$ between treatments.

flux rate in the two strains declined with increasing duration of hydroponic culture regardless of control and Cd^{2+} treatments (**Figure 3**). Non-inoculated *P.* × *canescens* roots exhibited a net Ca^{2+} influx under unstressed control conditions and the Ca^{2+} influx was stimulated by 7 days inoculation with MAJ and NAU (Supplementary Figure S1B). ST-treated *P. involutus*-inoculated roots retained higher Ca^{2+} influx than non-inoculated roots although the Ca^{2+} influx in poplar roots was lowered by Cd^{2+} stress (Supplementary Figure S1B).

It has been suggested that the Ca^{2+} enrichment in EM roots was associated with the *P. involutus* fungal hyphae exhibiting a high capacity for Ca^{2+} uptake (**Figures 1B** and **3**; Li J. et al., 2012; Ma X. et al., 2014). However, the Ca^{2+} influx in EM roots was not evidently correlated to the flux rate of Ca^{2+} in fungal hyphae under Cd^{2+} shock, ST, or LT (Supplementary Figure S3). Unexpectedly, the Ca^{2+} flux in EM roots was even negatively correlated to the flux rate of Ca^{2+} in fungal hyphae after a shock treatment (Supplementary Figure S3). The observed correlation of Ca^{2+} fluxes between EM roots and NM roots (Supplementary Figure S3) supports that the Ca^{2+} flow was mainly the consequence of host roots in the Cd^{2+}-stressed ectomycorrhizal symbioses.

FIGURE 2 | Effects of CdCl$_2$ on steady Cd^{2+} fluxes in *Populus* × *canescens* roots and *Paxillus involutus* strains MAJ and NAU. *P. involutus* isolates, ectomycorrhizal (MAJ and NAU) and non-mycorrhizal (NM) *P.* × *canescens* plants were subjected to short-term (ST, 24 h) and long-term (LT, 7 d) exposure to 50 μM CdCl$_2$, respectively. Control roots and axenic mycelia were well fertilized but treated without CdCl$_2$. Cd^{2+} fluxes in poplar roots were measured along root axis, 100–2,300 μm from the apex, at intervals of 200–300 μm. Cd^{2+} fluxes of *P. involutus* isolates MAJ and NAU were measured along the surface of pelleted hyphae over a recording period of 30 min. Inserted sections show the Cd^{2+} fluxes in *P. involutus* isolates after short-term (ST, 24 h) or long-term (LT, 7 days) CdCl$_2$ treatment. Each point is the mean of 4–5 individual plants or axenic EM cultures (pelleted hyphae), and bars represent the standard error of the mean. Asterisks denote significant difference at $P < 0.05$ between treatments.

FIGURE 3 | Effects of CdCl$_2$ on steady Ca^{2+} fluxes in *Populus* × *canescens* roots and *Paxillus involutus* strains MAJ and NAU. *P. involutus* isolates, ectomycorrhizal (MAJ and NAU) and non-mycorrhizal (NM) *P.* × *canescens* plants were subjected to short-term (ST, 24 h) and long-term (LT, 7 days) exposure to 50 μM CdCl$_2$, respectively. Control roots and axenic mycelia were well fertilized but treated without CdCl$_2$. Ca^{2+} fluxes in poplar roots were measured along root axis, 100–2,300 μm from the apex, at intervals of 200–300 μm. Ca^{2+} fluxes of *P. involutus* isolates MAJ and NAU were measured along the surface of pelleted hyphae over a recording period of 30 min. Inserted sections show the Ca^{2+} fluxes in *P. involutus* isolates after short-term (ST, 24 h) or long-term (LT, 7 days) CdCl$_2$ treatment. Each point is the mean of 4–5 individual plants or axenic EM cultures (pelleted hyphae), and bars represent the standard error of the mean. Asterisks denote significant difference at $P < 0.05$ between treatments.

Correlations between Cd^{2+} and Ca^{2+} Fluxes

We analyzed the correlation between Cd^{2+} and Ca^{2+} fluxes as NM and EM roots took up these elements with a similar flux rate (**Figures 1A,B**, **2** and **3**). Under ST and LT stress conditions, the total flux rates of Cd^{2+} and Ca^{2+} in the presence of Cd^{2+} ($=\Sigma_{Ca^{2+}+Cd^{2+}}$ with a molar ratio of Cd^{2+} to Ca^{2+} of 1:1) were 37.8–77.4 (NM), 54.1–96.2 (MAJ), and 53.7–122.1 pmol cm^{-2} s^{-1} (NAU), as calculated on the basis of **Figures 2** and **3** (Supplementary Figure S4). The relationships between $\Sigma_{Ca^{2+}+Cd^{2+}}$ and Ca^{2+} flux in the absence of $CdCl_2$ $[\Sigma_{Ca^{2+}(-Cd^{2+})}]$ were highly significant and close to 1 for NM and MAJ colonized roots and slightly increased to 1.4 for NAU colonized roots (**Figure 4**). These suggest that the entry of Cd^{2+} and Ca^{2+} is mainly through the same pathway in NM and EM roots, mostly likely through Ca^{2+}-permeable channels in the PM (see below).

H^+ Fluxes

In the absence of $CdCl_2$, EM roots showed a typical H^+ efflux at the apex, which was 7.6-fold higher than that in NM roots (**Figure 1C**). $CdCl_2$ (50 µM) shock stimulated H^+ efflux in both NM and EM plants with a stronger response in EM than in NM roots (**Figure 1C**). Pure MAJ and NAU mycelia exhibited a net H^+ efflux under control conditions similar to that observed for MAJ- and NAU-colonizing roots (**Figure 1C**). However, in pure mycelia the fluxes were 4.8-fold higher than in EM roots (**Figure 1C**). After exposure to $CdCl_2$ (50 µM), hyphae exhibited a transient increase in the H^+ efflux, which then remained constant during the period of recording (40 min; **Figure 1C**). Compared with strain MAJ, strain NAU exhibited higher H^+ efflux irrespective of control or $CdCl_2$ shock treatments (**Figure 1C**).

Steady-state recordings on EM roots showed that the pattern of H^+ flux in ST-stressed roots (50 µM $CdCl_2$, 24 h) differed from those subjected to LT Cd^{2+} exposure (50 µM $CdCl_2$, 7 days). Under ST conditions, $CdCl_2$ (50 µM) stimulated H^+ efflux in EM plants, whereas under LT conditions, EM roots showed a pronounced H^+ influx (**Figure 5**). In NM roots, $CdCl_2$ (50 µM) decreased H^+ influx upon ST exposure or shifted it to a net H^+ efflux under LT stress conditions (**Figure 5**). The pattern of H^+ flux in the fungal mycelia differed from that in EM roots under ST stress (**Figure 5**). ST treatment reduced the efflux of H^+ from the two fungal strains, which is contrast to EM roots where an enhanced H^+ efflux was observed (**Figure 5**). LT stress caused a pronounced shift of H^+ efflux to influx into pure mycelia of the two strains, similar to the finding in LT-stressed EM roots (**Figure 5**).

Cd^{2+}-Altered Flux Profiles of H_2O_2 in EM Roots

H_2O_2-sensitive microprobes were used to detect the H_2O_2 response to Cd^{2+} exposure in NM and EM roots. In the absence of Cd^{2+}, NM roots exhibited a stable H_2O_2 efflux (0.7–1.5 pmol cm^{-2} s^{-1}) along the root axis; the mean flux rate increased 2.4-fold in response to Cd^{2+} treatment (50 µM $CdCl_2$, 30 min, **Figure 6**). Ectomycorrhization of poplar roots with *P. involutus*
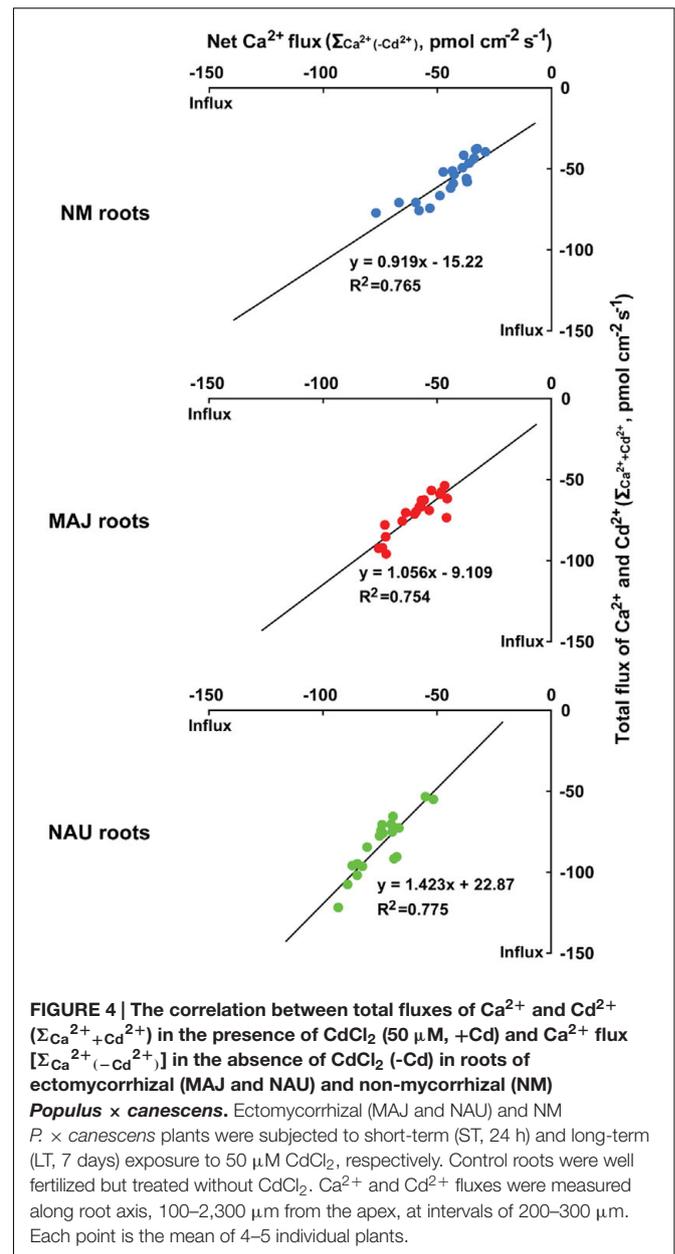
FIGURE 4 | The correlation between total fluxes of Ca^{2+} and Cd^{2+} ($\Sigma_{Ca^{2+}+Cd^{2+}}$) in the presence of $CdCl_2$ (50 µM, +Cd) and Ca^{2+} flux [$\Sigma_{Ca^{2+}(-Cd^{2+})}$] in the absence of $CdCl_2$ (-Cd) in roots of ectomycorrhizal (MAJ and NAU) and non-mycorrhizal (NM) *Populus* x *canescens*. Ectomycorrhizal (MAJ and NAU) and NM *P.* x *canescens* plants were subjected to short-term (ST, 24 h) and long-term (LT, 7 days) exposure to 50 µM $CdCl_2$, respectively. Control roots were well fertilized but treated without $CdCl_2$. Ca^{2+} and Cd^{2+} fluxes were measured along root axis, 100–2,300 µm from the apex, at intervals of 200–300 µm. Each point is the mean of 4–5 individual plants.

stains, MAJ and NAU, resulted in a significant increase of H_2O_2 efflux along the roots (**Figure 6**). However, upon $CdCl_2$ exposure EM roots displayed decreased H_2O_2 efflux in contrast to NM roots (**Figure 6**).

Effects of Ca^{2+}, H_2O_2, pH, and PM Transporter and Channel Inhibitors on Cd^{2+}-Altered Ion Flux Profiles in EM Roots

Ca^{2+} and Ca^{2+} Channel Inhibitors

Here, pharmacological experiments were carried out to test whether putative Ca^{2+} channels inhibitors could inhibit Cd^{2+} influx in poplar roots. Four typical Ca^{2+} channels
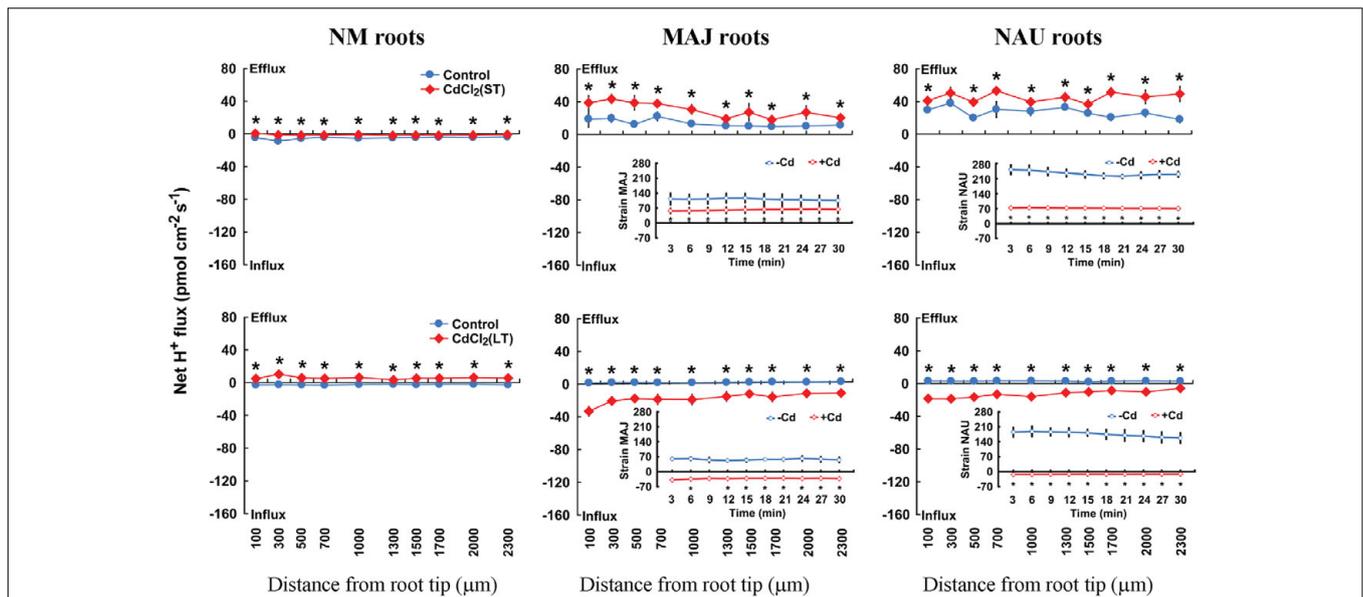
FIGURE 5 | Effects of CdCl₂ on steady H⁺ fluxes in *Populus* × *canescens* roots and *Paxillus involutus* strains MAJ and NAU. *P. involutus* isolates, ectomycorrhizal (MAJ and NAU) and non-mycorrhizal (NM) *P.* × *canescens* plants were subjected to short-term (ST, 24 h) and long-term (LT, 7 days) exposure to 50 µM CdCl₂, respectively. Control roots and axenic mycelia were well fertilized but treated without CdCl₂. H⁺ fluxes in poplar roots were measured along root axis, 100–2,300 µm from the apex, at intervals of 200–300 µm. H⁺ fluxes of *P. involutus* isolates MAJ and NAU were measured along the surface of pelleted hyphae over a recording period of 30 min. Inserted sections show the H⁺ fluxes in *P. involutus* isolates after short-term (ST, 24 h) or long-term (LT, 7 days) CdCl₂ treatment. Each point is the mean of 4–5 individual plants or axenic EM cultures (pelleted hyphae), and bars represent the standard error of the mean. Asterisks denote significant difference at $P < 0.05$ between treatments.
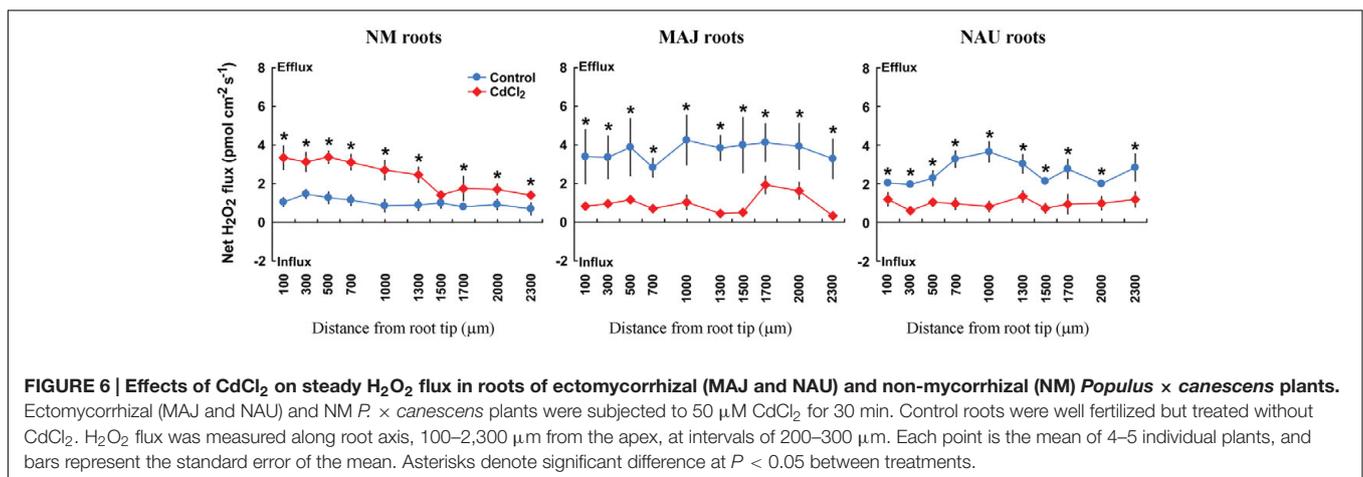
FIGURE 6 | Effects of CdCl₂ on steady H₂O₂ flux in roots of ectomycorrhizal (MAJ and NAU) and non-mycorrhizal (NM) *Populus* × *canescens* plants. Ectomycorrhizal (MAJ and NAU) and NM *P.* × *canescens* plants were subjected to 50 µM CdCl₂ for 30 min. Control roots were well fertilized but treated without CdCl₂. H₂O₂ flux was measured along root axis, 100–2,300 µm from the apex, at intervals of 200–300 µm. Each point is the mean of 4–5 individual plants, and bars represent the standard error of the mean. Asterisks denote significant difference at $P < 0.05$ between treatments.

inhibitors, LaCl₃, GdCl₃, verapamil, and TEA effectively inhibited Ca^{2+} influx in NM and EM roots, regardless of Cd^{2+} treatments (**Figure 7A**, Supplementary Figures S5A, S6A, and S7A). LaCl₃ restricted Cd^{2+} influx in CdCl₂-treated NM and EM roots (**Figure 7B**). This suggests that Cd^{2+} is taken up through Ca^{2+}-permeable channels because La^{3+} is able to block various types of Ca^{2+}-permeable channels, including depolarisation-, hyperpolarisation-, elicitor-activated, and voltage-insensitive channels (Weiss, 1974; Pickard and Ding, 1993; Gelli and Blumwald, 1997; Piñeros and Tester, 1997; Zimmermann et al., 1997; White, 1998, 2000). Moreover, the other three Ca^{2+}-permeable channel

inhibitors, GdCl₃, verapamil, and TEA, diminished Cd^{2+} influx to a similar extent as LaCl₃-treated plants (**Figure 7B**, Supplementary Figures S5B, S6B, and S7B). Similarly, in the pure *P. involutus* mycelia, LaCl₃ also effectively restricted influx of Ca^{2+} and Cd^{2+} or induced net efflux (Supplementary Figure S8).

Additionally, a co-application of Cd^{2+} and Ca^{2+} suppressed the entry of Cd^{2+} in NM and EM roots, and the restriction increased with the increasing fraction of Ca^{2+} in the mixture (Ca^{2+}: Cd^{2+} = 1:2, 1:1, 2:1; **Figure 7C**). The mean Cd^{2+} flux decreased by 95.7% (NM), 72.1% (MAJ), and 45.5% (NAU) at a ratio of Ca^{2+}:Cd^{2+} = 2:1, compared to a those with a higher

FIGURE 7 | Effects of LaCl$_3$ and external Ca^{2+} on steady Cd^{2+} and/or Ca^{2+} fluxes in roots of ectomycorrhizal (MAJ and NAU) and non-mycorrhizal (NM) *Populus* × *canescens* **plants under Cd^{2+} stress. (A,B)** Ectomycorrhizal (MAJ and NAU) and NM *P.* × *canescens* plants were subjected to 50 µM CdCl$_2$ for 24 h in the presence and absence of 5 mM LaCl$_3$. Control roots were well fertilized but treated without CdCl$_2$ or LaCl$_3$. **(C)** Ectomycorrhizal (MAJ and NAU) and NM *P.* × *canescens* plants were subjected to 50 µM CdCl$_2$ for 24 h prior to Cd^{2+} flux recordings in the presence of CaCl$_2$ (25 µM, 50 µM, or 100 µM; the ratio of Ca^{2+}:Cd^{2+} was 1:2; 1:1, and 2:1). Ca^{2+} **(A)** and Cd^{2+} **(B,C)** fluxes were measured along root axes, 100–2,300 µm from the apex, at intervals of 200–300 µm. Each point is the mean of 4–5 individual plants and bars represent the standard error of the mean. Inserted sections show the mean flux rates and different letters, a, b, c, and d, indicate significant difference at $P < 0.05$ between treatments.

Cd^{2+} fraction, Ca^{2+}:Cd^{2+} = 1:2 (**Figure 7C**). These results suggest that the divalent cations, Cd^{2+} and Ca^{2+}, competitively permeated the plasma membrane through Ca^{2+} channels. The lower reduction in Cd^{2+} influx in EM than in NM roots in the presence of Ca^{2+} (**Figure 7C**) reflects the high flow of Cd^{2+} through the activated Ca^{2+} channels.

We observed that the presence of Ca^{2+} in the measuring solution marginally lowered the Cd^{2+} signals (14.7–26.0%) detected by the Cd^{2+} microelectrodes filled with Cd^{2+} liquid ion exchanger (LIX) (Supplementary Table S1). In the absence of Ca^{2+}, the working voltage of microelectrodes and the detected Cd^{2+} signals in Cd^{2+}-treated roots were unstable and fluctuated greatly during the period of recording (data not shown). This behavior is presumably caused by the plant response to nutrient deficiency in the root medium (Li J. et al., 2012). In our study, Cd^{2+} electrodes exhibited higher sensitivity at 0.05 mM Ca^{2+} in the absence and presence of 0.1 mM K$^+$ and 0.1 mM Mg^{2+} (Supplementary Table S1). The presence of nutrients, K$^+$, Ca^{2+}, and Mg^{2+}, did not affect the accuracy of our conclusions relating to Cd^{2+} fluxes in NM and EM roots.

H$_2$O$_2$ and ROS Scavenger

To investigate whether Cd^{2+} entry through Ca^{2+}-permeable channels is activated by H$_2$O$_2$, we examined the effects of hydrogen peroxide and the ROS (reactive oxygen species) scavenger DMTU on Cd^{2+} and Ca^{2+} fluxes. Transient kinetic recordings showed that Cd^{2+} shock caused an immediate increase of Cd^{2+} influx but enhanced Ca^{2+} efflux in NM and EM roots (**Figure 8**). The flux rates of Cd^{2+} and Ca^{2+} decreased with prolonged exposure time (**Figure 8**). Notably, Cd^{2+} influx markedly increased upon H$_2$O$_2$ shock (1.0 mM) in both NM and EM roots (**Figure 8A**). However, the Cd^{2+}-elicited Ca^{2+} efflux was reduced by H$_2$O$_2$ in EM roots or shifted to a net influx in NM roots (**Figure 8B**). These results suggest that H$_2$O$_2$ stimulated the entry of Cd^{2+} and Ca^{2+}, presumably through the plasma membrane Ca^{2+} channels of the roots.

Ca^{2+} influx in NM and EM roots were suppressed by the ROS scavenger, DMTU (5 mM), irrespective of the presence and absence of Cd^{2+} (**Figure 9A**). Similarly, the supplement of DMTU significantly reduced the influx of Cd^{2+} in NM and EM roots (**Figure 9B**). These data indicated that H$_2$O$_2$ play a crucial role in accelerating the influx of Ca^{2+} and Cd^{2+}, which
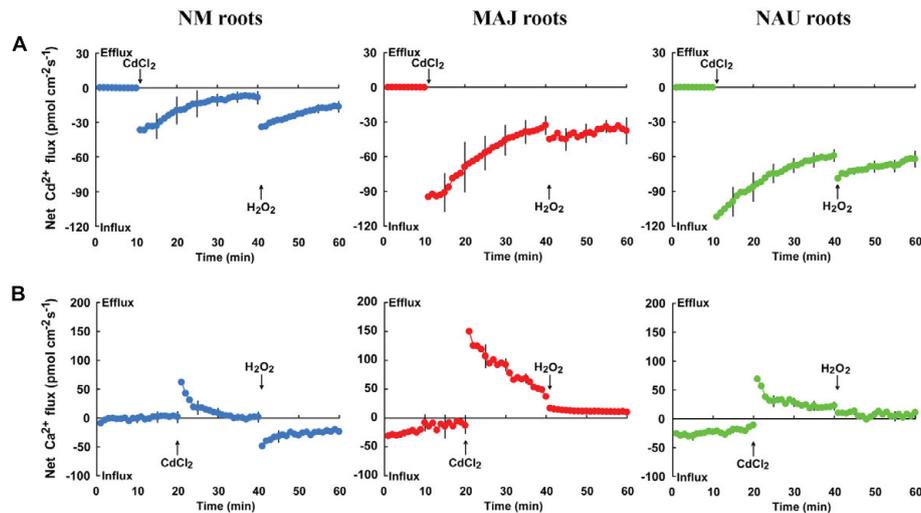
FIGURE 8 | Effects of CdCl$_2$ and H$_2$O$_2$ on transient kinetics of Cd^{2+} and Ca^{2+} in roots of ectomycorrhizal (MAJ and NAU) and non-mycorrhizal (NM) *Populus* × *canescens*. Cd^{2+} **(A)** and Ca^{2+} **(B)** kinetics were recorded before and after the required amount of 50 μM CdCl$_2$ or 1.0 mM H$_2$O$_2$ was introduced into the measuring chamber. Prior to the CdCl$_2$ shock, steady-state fluxes of Cd^{2+} and Ca^{2+} were monitored at the apex (measuring site was ca. 100 μm from the root tip) for approximately 10–20 min. Transient kinetics of Cd^{2+} and Ca^{2+} were recorded after the required amount of 50 μM CdCl$_2$ was introduced into the measuring solution. After 20–30 min continuous recording of Cd^{2+} and Ca^{2+} fluxes, Cd^{2+} and Ca^{2+} kinetics were recorded for 20 min after 1.0 mM H$_2$O$_2$ was introduced into the measuring solution. Each point represents the mean of 4–5 individual plants and bars represent the standard error of the mean.
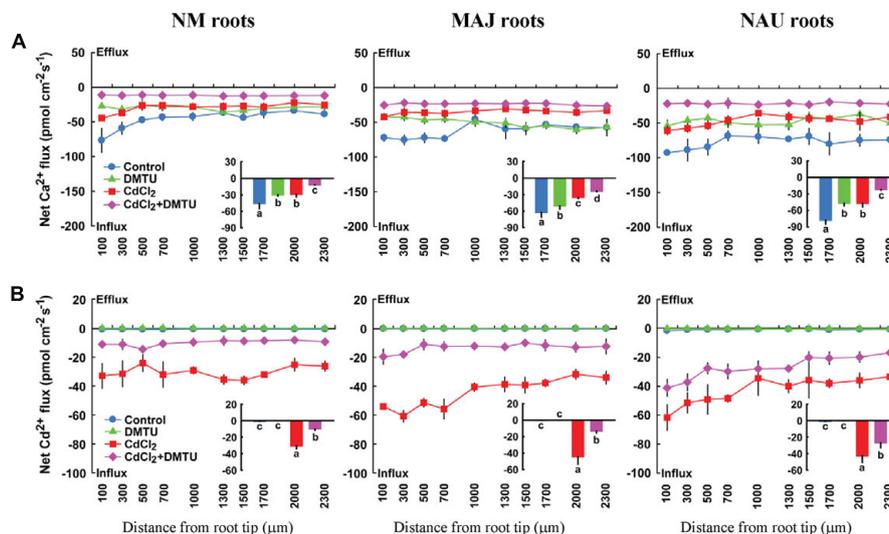
FIGURE 9 | Effects of DMTU on steady Ca^{2+} and Cd^{2+} fluxes in roots of ectomycorrhizal (MAJ and NAU) and non-mycorrhizal (NM) *Populus* × *canescens* under Cd^{2+} stress. Ectomycorrhizal (MAJ and NAU) and NM *P.* × *canescens* plants were subjected to 0 or 50 μM CdCl$_2$ for 24 h in the presence or absence of 5 mM DMTU. Ca^{2+} **(A)** and Cd^{2+} **(B)** fluxes were measured along root axes, 100–2,300 μm from the apex, at intervals of 200–300 μm. Each point is the mean of 4–5 individual plants and bars represent the standard error of the mean. Inserted sections show the mean flux rates and different letters, a, b, c, and d, indicate significant difference at $P < 0.05$ between treatments.

is accordance to the results obtained by direct H$_2$O$_2$ applications (**Figure 8**).

External pH and H$^+$-ATPase Inhibitor

Fluxes of Cd^{2+} and Ca^{2+} depend on external pH. An acidic environment accelerated Cd^{2+} and Ca^{2+} influxes in both NM and EM roots with the strongest influx at pH 5.2 and the

lowest at pH 6.2 or a neutral pH, 7.2 (**Figure 10**). Moreover, we noticed that the pH effects on fluxes of Cd^{2+} and Ca^{2+} were more pronounced in NM roots than in EM roots (**Figure 10**). Compared to an acidic environment (pH 5.2), the mean flux rate of the divalent cations decreased by 45.8% (Ca^{2+}) and 38.8% (Cd^{2+}) in EM roots under pH 6.2–7.2 (**Figure 10**). In NM roots, the increasing pH lowered Cd^{2+} influxes by 56.5% or even
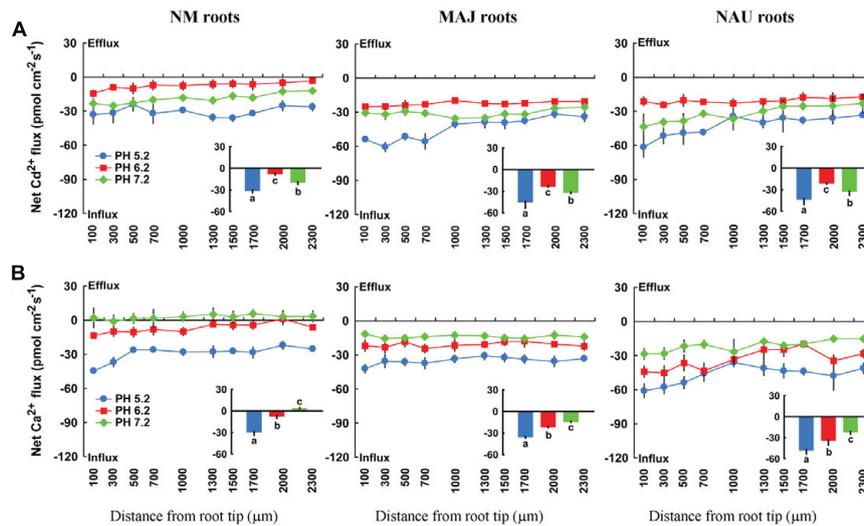
FIGURE 10 | Effects of pH on steady Cd^{2+} and Ca^{2+} fluxes in roots of ectomycorrhizal (MAJ and NAU) and non-mycorrhizal (NM) *Populus* × *canescens* under Cd^{2+} stress. Ectomycorrhizal (MAJ and NAU) and NM *P.* × *canescens* plants were subjected to 50 μM $CdCl_2$ for 24 h prior to flux recordings at pH 5.2, 6.2 or 7.2. Cd^{2+} **(A)** and Ca^{2+} **(B)** fluxes were measured along root axes, 100–2,300 μm from the apex, at intervals of 200–300 μm. Each point is the mean of four to five individual plants and bars represent the standard error of the mean. Inserted sections show the mean flux rates and different letters, a, b, and c, indicate significant difference at $P < 0.05$ between treatments.

reversed the rectifications of Ca^{2+} (influx → efflux) at a neutral pH, 7.2 (**Figure 10**). The less reduced influx of Ca^{2+} and Cd^{2+} in EM roots at pH 6.2 or 7.2 was due to the high H^+-pumping activity in the PM (see below).

Sodium orthovanadate (500 μM), the specific inhibitor of PM H^+-ATPase, increased the H^+ influx in NM roots slightly, but caused a drastic shift from H^+ efflux toward influx in both EM roots and *P. involutus* mycelia, irrespective of Cd^{2+} treatment (**Figure 11A**, Supplementary Figure S9). Sodium orthovanadate significantly reduced the Cd^{2+} influx along the roots in Cd^{2+}-treated NM and EM plants (**Figure 11B**). In the absence of Cd^{2+}, the PM H^+-ATPase inhibitor reduced Ca^{2+} influx in NM and MAJ-ectomycorrhizal roots or shifted to efflux in NAU-ectomycorrhizal roots (**Figure 11C**). The inhibition of Ca^{2+} influx by sodium orthovanadate was more pronounced in the presence of Cd^{2+}: the H^+-pump inhibitor reversed the rectifications of Ca^{2+} from influx to efflux in NM and EM roots (**Figure 11C**).

DISCUSSION

Colonization of *P.* × *canescens* Roots with *Paxillus involutus* Stimulates Cd^{2+} Uptake under Cd^{2+} Stress

The woody Cd^{2+}-hyperaccumulator *P.* × *canescens* exhibited a vigorous Cd^{2+} uptake after a 50 μM $CdCl_2$ shock (40 min), ST (24 h), and LT (7 days) treatment (**Figures 1A** and **2**). The result is consistent with previous findings where *P.* × *canescens* roots exhibited a high Cd^{2+} uptake after 40 days of $CdSO_4$ exposure (50 μM, Ma Y. et al., 2014). Similarly, a high entry of Cd^{2+} was

recorded in hyperaccumulating ecotypes of *Sedum alfredii* (Lu et al., 2010; Sun et al., 2013a) and *Suaeda salsa* under Cd^{2+} stress (Li et al., 2012a). An important result was that EM roots exhibited higher Cd^{2+} influx than NM roots irrespective of Cd^{2+} stress conditions, shock, ST, and LT (**Figures 1A** and **2**). Substantial evidence indicates that Cd^{2+} can be enriched in ectomycorrhizal plants (Sell et al., 2005; Baum et al., 2006; Krpata et al., 2008, 2009; Sousa et al., 2012; Ma Y. et al., 2014). The enhanced Cd^{2+} uptake in EM roots is partly due to the capacity of the fungus to take up Cd^{2+} because $CdCl_2$ shock resulted in a net Cd^{2+} influx in the mycelia of the two *P. involutus* strains and the flux rate increased with the prolonged duration of $CdCl_2$ treatment from 24 h to 7 days (**Figures 1A** and **2**). In liquid cultures, *P. involutus* cultures also showed high capacities for Cd^{2+} accumulation (Ott et al., 2002). *P. involutus* could bind Cd^{2+} onto the cell walls or accumulate the metal in the vacuolar compartment (Blaudez et al., 2000; Ott et al., 2002). Moreover, the ectomycorrhizal fungus appears to detoxify high concentrations of Cd^{2+} by (i) the chelation of metal ions in the cytosol with thiol-containing compounds, e.g., glutathione, phytochelatins, or metallothioneins (Courbot et al., 2004; Jacob et al., 2004), and (ii) activation of antioxidative defense system (Jacob et al., 2001; Ott et al., 2002). Our pharmacological data revealed that Cd^{2+} entered the fungal hyphae mainly through PM Ca^{2+} channels because the influx was suppressed by $LaCl_3$, a Ca^{2+} channel blocker (Supplementary Figure S8B). Therefore, Cd^{2+} enriched by ectomycorrhizal hyphae is thought to be transferred to the host roots, probably through the apoplastic space during the period of Cd^{2+} stress.

There were marked differences between the two strains in Cd^{2+} uptake given the shock treatment (**Figure 1A**). Pure fungal mycelium of MAJ accumulated Cd^{2+} with a higher rate
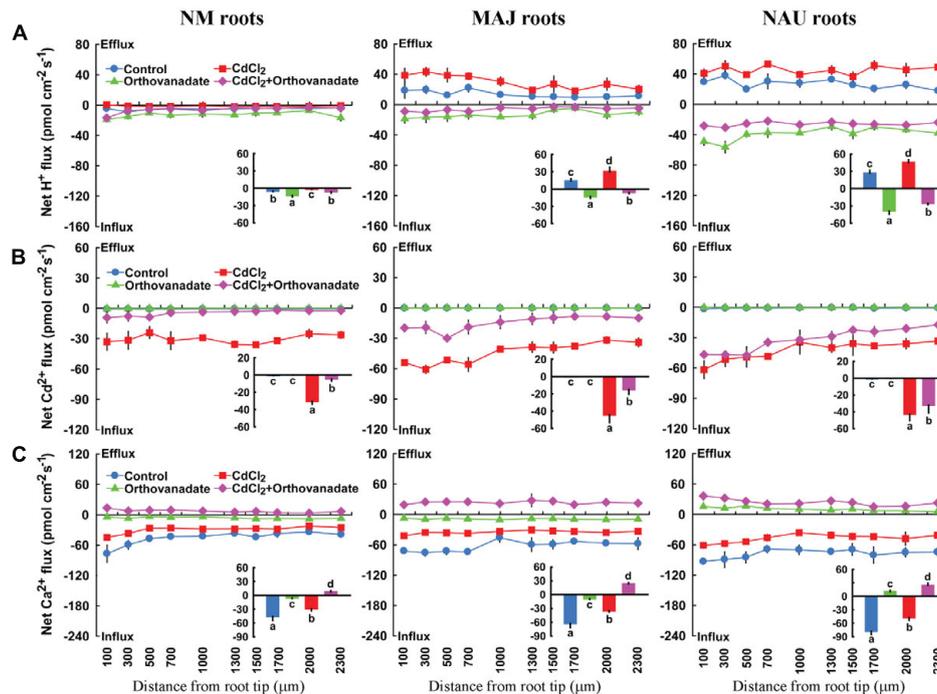
FIGURE 11 | Effects of sodium orthovanadate on steady H$^+$, Cd^{2+}, and Ca^{2+} fluxes in roots of ectomycorrhizal (MAJ and NAU) and non-mycorrhizal (NM) *Populus × canescens* **under Cd^{2+} stress.** Ectomycorrhizal (MAJ and NAU) and NM *P. × canescens* plants were subjected to 0 or 50 µM CdCl$_2$ for 24 h in the presence and absence of 500 µM sodium orthovanadate. H$^+$ **(A)**, Cd^{2+} **(B)**, and Ca^{2+} **(C)** fluxes were measured along root axes, 100–2,300 µm from the apex, at intervals of 200–300 µm. Each point is the mean of 4–5 individual plants and bars represent the standard error of the mean. Inserted sections show the mean flux rates and different letters, a, b, c, and d, indicate significant difference at *P* < 0.05 between treatments.

than NAU (**Figure 1A**). In the *P. involutus*-ectomycorrhizal symbioses, the incompatible fungal isolate NAU is unable to induce a functional ectomycorrhizae while MAJ forms a typical Hartig net with the roots of *P. × canescens* (Gafur et al., 2004). Thus, in MAJ-colonized roots the host cells might have been more accessible to Cd^{2+}. In accordance, MAJ roots exhibited a higher influx than NAU roots after the onset of CdCl$_2$ shock (**Figure 1A**). However, Cd^{2+} influx into NAU-colonized roots was similar to that of MAJ-colonized roots during ST or LT Cd^{2+} treatment (**Figure 2**). This was likely due to (i) similar capacities for Cd^{2+} uptake of MAJ and NAU hyphae during a 24-h or 7-days of Cd^{2+} exposure (**Figure 2**), or (ii) similar uptake capacity of the fungus-ensheathed inner root cells (**Figure 2**). The observed correlation between EM and NM roots showed that the continuous Cd^{2+} flow was mainly the consequence of host roots in the Cd^{2+}-stressed ectomycorrhizal symbioses during a prolonged period of Cd^{2+} exposure (24 h to 7 days; Supplementary Figure S2).

Paxillus involutus-Ectomycorrhizas Enhance Cd^{2+} Influx through Ca^{2+}-Permeable Channels in the Plasma Membrane

Our data revealed that the entry of Cd^{2+} is likely mediated through PM Ca^{2+} channels in the fungal hyphae and poplar

roots, and *P. involutus*-ectomycorrhizas facilitated the channel-mediated Cd^{2+} influx under Cd^{2+} stress. The experimental evidence for these conclusions is briefly listed below.

(1) The addition of Cd^{2+} resulted in an immediate influx of Cd^{2+} in NM roots, and the flux was more pronounced in EM roots (**Figure 1A**). Rapid entry of Cd^{2+} is generally through PM ion channels that are permeable to Cd^{2+} (The first 1–2 min flux recordings were discarded to diminish the diffusion effect of stock addition in roots and fungal mycelia). Our pharmacological data revealed that the net Cd^{2+} influx in CdCl$_2$-stressed NM and EM roots was strongly suppressed by typical Ca^{2+} channel blockers, such as LaCl$_3$, GdCl$_3$, verapamil, and TEA (**Figure 7B**, Supplementary Figures S5B, S6B, and S7B). Moreover, in *P. involutus* mycelium the CdCl$_2$-elicited influx of Cd^{2+} was also inhibited by LaCl$_3$ (Supplementary Figure S8B). These results suggest that under CdCl$_2$ stress Cd^{2+} enters fungal and root tissues through PM Ca^{2+} channels.

(2) Cd^{2+} treatments (shock, ST, and LT) affected the uptake of Ca^{2+} in poplar roots (**Figures 1B** and **3**), while the influx of Cd^{2+} declined with increasing the concentration of Ca^{2+} when NM and EM roots were subjected to the concomitant application of Cd^{2+} and Ca^{2+} (**Figure 7C**). Similarly, the Cd^{2+} influx was affected by the presence of Ca^{2+} in two contrasting (hyperaccumulating and

non-hyperaccumulating) *Sedum alfredii* ecotypes (Lu et al., 2010). It was suggested that Ca^{2+} and Cd^{2+} ions compete for the binding sites of transporters (Gussarsson et al., 1996; Rodríguez-Serrano et al., 2009). Our transient kinetics showed that Cd^{2+} exposure blocked the Ca^{2+} influx and caused an immediate change in the rectification of Ca^{2+} from influx to efflux (**Figures 1B** and **8B**). This suggests that Cd^{2+} ions competed with Ca^{2+} to penetrate across PM Ca^{2+} channels that are permeable to divalent cations (Perfus-Barbeoch et al., 2002).

(3) In ST- and LT-stressed NM and EM roots, the total flux rates of Cd^{2+} and Ca^{2+} in the presence of Cd^{2+} ($\Sigma_{Ca^{2+}+Cd^{2+}}$) were nearly equal to the flux rate of Ca^{2+} in the absence of Cd^{2+} stress ($\Sigma_{Ca^{2+}(-Cd^{2+})}$; Supplementary Figure S4). Moreover, the correlations between $\Sigma_{Ca^{2+}+Cd^{2+}}$ and $\Sigma_{Ca^{2+}(-Cd^{2+})}$ (**Figure 4**) suggest that Cd^{2+} ions enter NM and EM roots mainly through Ca^{2+}-permeable channels in the PM.

Collectively, under $CdCl_2$ stress Cd^{2+} ions could penetrate the PM Ca^{2+} channels in fungal hyphae and in *P.* × *canescens* roots. At present we cannot exclude the possibility that Cd^{2+} penetrated the PM through transporters for Cd^{2+} (Ma Y. et al., 2014; He et al., 2015) or other nutritional ions (Gussarsson et al., 1996; Cohen et al., 1998; Zhao et al., 2002; Cosio et al., 2004; Clemens, 2006), because (1) the four types of Ca^{2+} channel inhibitors applied here were not able to fully block the Cd^{2+} influx in NM and EM roots (**Figure 7B**, Supplementary Figures S5B, S6B and S7B), and (2) the total flux of Cd^{2+} and Ca^{2+} ($\Sigma_{Ca^{2+}+Cd^{2+}}$, molar ratio of Cd^{2+} to Ca^{2+} is 1:1) under ST and LT Cd^{2+} stress was 10.9–27.7% higher than the flux rate of Ca^{2+} under non-Cd^{2+} conditions (**Figure 4**, Supplementary Figure S4). This implies that a small fraction of Cd^{2+} ions penetrated the PM through other channels and transporters.

Plasma membrane Ca^{2+} channels in *P. involutus* hyphae maybe more permeable to Cd^{2+} compared to the channels in *P.* × *canescens* roots as the fungal mycelium displayed a typical higher Ca^{2+} influx than poplar roots under control and Cd^{2+}-stress conditions (**Figures 1B** and **3**). We cannot discriminate between the channels of the fungus and those of the plant in the ectomycorrhizal symbiosis, but the Cd^{2+} and Ca^{2+} fluxes in EM roots appear to mainly reflect the response of the host plants to Cd^{2+} stress because (1) EM roots exhibited a different pattern from the *P. involutus* mycelia in enhancing Ca^{2+} and Cd^{2+} uptake under hydroponic Cd^{2+} conditions. Cd^{2+}-shocked MAJ and NAU fungal strains usually displayed a stable Cd^{2+} influx with the exception of an initial transient increase (**Figure 1A**). However, EM roots showed a declined Cd^{2+} influx over the duration of Cd^{2+} exposure, similar to the Cd^{2+} kinetics in NM roots (**Figure 1A**). Moreover, the Cd^{2+} influx in the mycelia of the two *P. involutus* strains increased with the prolonged $CdCl_2$ exposure from 24 h to 7 days (from 23.9 to 72.7 pmol cm^{-2} s^{-1}; **Figure 2**). In contrast, the Cd^{2+} fluxes in EM roots were relatively stable under ST (43.7 ± 8.4 pmol cm^{-2} s^{-1}) and LT treatments (35.9 ± 6.0 pmol cm^{-2} s^{-1}; **Figure 2**). ST, LT, and Cd^{2+} shock increased the Ca^{2+} influx in *P. involutus* mycelia, while the

Ca^{2+} influx in EM roots was declined by these Cd^{2+} treatments (**Figures 1B** and **3**). (2) NMT data showed that ion fluxes in mature *P.* × *canescens*–*P. involutus* symbiotic associations bear a striking resemblance to the ST inoculated roots (Supplementary Figure S1). Similar findings have been previously reported in a salt stress study where *P.* × *canescens* roots were inoculated with *P. involutus* for 10 and 20 days (Ma X. et al., 2014). At early stages of fungal co-culture the Cd^{2+} and Ca^{2+} influx is mostly the result of host properties. Therefore, the Cd^{2+} and Ca^{2+} stimulation in *P. involutus*-ectomycorrhizal roots reflects the enhanced root uptake ability. (3) The correlation analyses revealed that Cd^{2+} and Ca^{2+} influxes in EM roots show a significant relationship with NM roots but not with fungal mycelia under various Cd^{2+} treatments (shock, ST, and LT; Supplementary Figures S2 and S3). Taken together, these data suggest that the continuous flow of Cd^{2+} and Ca^{2+} in EM roots detected by NMT microelectrodes was largely driven by the host and that the fungal partner enhanced fluxes leading to enriched Cd^{2+} and Ca^{2+} concentrations.

The observed patterns of Cd^{2+} and Ca^{2+} fluxes upon Cd^{2+} exposure could be explained by channel-mediated ion fluxes. NMT data show that the Ca^{2+} flux in EM roots was negatively correlated with the Ca^{2+} influx in fungal hyphae upon Cd^{2+} shock treatment (Supplementary Figure S3). This is presumably the result of Cd^{2+}-Ca^{2+} competition across the Ca^{2+} channels in the root PM. After being exposed to Cd^{2+} shock, Ca^{2+} entry was enhanced in the hyphae (**Figure 1B**). However, the fungal hyphae which were enriched in Ca^{2+} ions, were unable to deliver Ca^{2+} to the root cells because the Cd^{2+} ions competitively inhibited the entry of Ca^{2+} through the PM channels. As a result, the high influx of Ca^{2+} through fungal hyphae led to an apparently greater Ca^{2+} efflux in Cd^{2+}-exposed EM roots (**Figures 1B** and **8B**).

Paxillus involutus colonization enhanced the uptake of Cd^{2+} under shock, ST, and LT stress, compared to NM roots (**Figures 1A** and **2**). The increased entry of Cd^{2+} is likely due to the activation of PM Ca^{2+} channels in the ectomycorrhizas. The stimulated Ca^{2+} influx by *P. involutus* inoculation revealed the activation of PM Ca^{2+} channels since the ectomycorrhiza-enhanced entry of Ca^{2+} was suppressed by Ca^{2+} channel blockers ($LaCl_3$, $GdCl_3$, verapamil, or TEA; **Figure 7A**, Supplementary Figures S5A, S6A, and S7A). The activated PM Ca^{2+} channels allowed the entry of Cd^{2+} in addition to Ca^{2+} under Cd^{2+} stress (**Figures 1A** and **2**).

Hydrogen Peroxide Induced by CdCl$_2$ and Fungal Colonization Stimulates Cd^{2+} Influx through PM Ca^{2+} Channels

After being subjected to $CdCl_2$ exposure, NM roots displayed an increased H_2O_2 efflux along the root axis (**Figure 6**). It is well documented that Cd^{2+} induced accumulation of H_2O_2 in pine roots (Schützendübel et al., 2001), *P.* × *canescens* roots (Schützendübel et al., 2002), and in suspension cultures of tobacco (Piqueras et al., 1999) and *P. euphratica* (Sun et al., 2013b; Han et al., 2016). H_2O_2 efflux was evident in EM roots irrespective of the presence or absence of Cd^{2+} treatments (**Figure 6**). Our results suggest that the Cd^{2+} influx through PM

Ca^{2+} channels is stimulated by H_2O_2 in NM and EM roots. The experimental evidence and explanations are briefly listed here.

(1) H_2O_2 (1.0 mM) exhibited an enhancement on Ca^{2+} influx in NM and EM roots (**Figure 8B**). Pei et al. (2000) showed that H_2O_2 (0.05–5.0 mM) activates Ca^{2+} currents through PM Ca^{2+} channels of *Arabidopsis thaliana* guard cells. Moreover, H_2O_2 increased Ca^{2+} influx across the PM in *P. euphratica* cells (Sun et al., 2010), roots of *A. thaliana* (Demidchik et al., 2007) and mangroves (Lu et al., 2013). Furthermore, the H_2O_2-stimulated entry of Ca^{2+} in *P. euphratica* cells was inhibited by $LaCl_3$ (Sun et al., 2010). In this study, Cd^{2+} influx in NM and EM roots was significantly enhanced after exposure to 1.0 mM H_2O_2 (**Figure 8A**). This finding is in agreement with Sun et al. (2013b) and Han et al. (2016), who found that H_2O_2 (3.0 mM) stimulated entry of Cd^{2+} into *P. euphratica* cells. In addition, the Cd^{2+} influx was blocked by $LaCl_3$ in $CdCl_2$-stressed roots (**Figure 7B**). These results suggest that H_2O_2 stimulates the influx of Cd^{2+} and Ca^{2+} through Ca^{2+}-permeable channels in the PM.

(2) The H_2O_2 induction of Cd^{2+} resembles the pattern of Ca^{2+} kinetics in response to H_2O_2 (**Figure 8**). Moreover, Cd^{2+} and Ca^{2+} influx in NM and EM roots were both suppressed by the ROS scavenger, DMTU (**Figure 9**). Similarly, Sun et al. (2013b) showed that the entry of Cd^{2+} into *P. euphratica* cells was reduced when a H_2O_2 scavenger, catalase, was applied.

Taken together, these results suggest that Cd^{2+} and Ca^{2+} ions enter NM and EM roots by the same pathway involving PM Ca^{2+} channels that are activated by Cd^{2+}-elicited H_2O_2.

The high Cd^{2+} influx in EM roots resulted from the pronounced activation of PM Ca^{2+} channels that were stimulated, at least in part, by the fungal-elicited H_2O_2. Compared to NM roots, MAJ- and NAU-ectomycorrhizal roots displayed a significant higher H_2O_2 efflux in the absence of Cd^{2+} stress (**Figure 6**), suggesting that the inoculation with *P. involutus* caused a strong production of H_2O_2 in EM roots. This finding agrees with Gafur et al. (2004) and Langenfeld-Heyser et al. (2007), who detected strong H_2O_2 accumulation in the outer hyphae mantle of compatible (MAJ) and incompatible (NAU) interactions. H_2O_2 production in the hyphae is suggested to regulate host's root growth, defense against other invading microbes, and increasing plant-innate immunity (Salzer et al., 1999; Gafur et al., 2004). In our study, H_2O_2 produced in the ectomycorrhizae accelerated the influx of Ca^{2+} in the absence of Cd^{2+}, whereas it increased entry of Cd^{2+} in the presence of high external Cd^{2+} (**Figure 8**). ROS scavenging by DMTU simultaneously decreased Ca^{2+} and Cd^{2+} influxes along the root axis of EM plants (**Figure 9**). These observations suggest that H_2O_2 produced in compatible (MAJ) and incompetent (NAU) ectomycorrhizal associations activated Ca^{2+} permeable channels, which allowed the entry of Cd^{2+} under Cd^{2+} stress.

We noticed that the H_2O_2 efflux in MAJ and NAU-ectomycorrhizal roots was lowered by Cd^{2+} stress (**Figure 6**). This reduction may have resulted from the activation of

antioxidant enzymes and increased amounts of ROS scavengers produced as a defense response. It has been repeatedly shown that the antioxidant enzyme activities are activated under heavy metal stresses (Schützendübel et al., 2001, 2002; Rozpądek et al., 2014; Chen et al., 2015; Tan et al., 2015). The enhanced activities of superoxide dismutase, peroxidase, catalase, and ascorbate peroxidase play an important role in scavenging the Cd^{2+}-elicited H_2O_2 in plants (Garg and Aggarwal, 2012; Anjum et al., 2015; Tan et al., 2015). To combat Cd^{2+}-induced superoxide and H_2O_2, *P. × canescens* plants were found to rely mainly on antioxidant enzymes and the formation of the potential radical scavenging molecules, such as proline, sugar alcohols and soluble phenolics (He et al., 2011). However, the lowered H_2O_2 efflux in EM roots (**Figure 6**) did not reduce the Cd^{2+}-elicited entry of Cd^{2+}, because (i) the fungal-elicited H_2O_2 had already activated the Ca^{2+}-channels before the Cd^{2+} addition, and/or (ii) the H_2O_2 level is still high enough to activate the channels under Cd^{2+} stress. The observation that stressed EM roots still contain high concentrations of H_2O_2 in the hyphae (Langenfeld-Heyser et al., 2007) supports these speculations.

PM H^+-ATPase Activated by Cd^{2+} and Fungal Colonization Stimulates Cd^{2+} Influx through PM Ca^{2+} Channels

In addition to H_2O_2, PM H^+-ATPase activated by Cd^{2+} and enhanced by fungal colonization also accelerated Cd^{2+} influx through PM Ca^{2+} channels in NM and EM roots. PM H^+-ATPases pump protons into the external medium to maintain an electrochemical H^+ gradient across the PM (Blumwald et al., 2000; Zhu, 2003). Krämer (2010) suggested that H^+-ATPases play an important role in adaptation of plants to heavy metal stress. The finding that the net H^+ efflux in fungal mycelia and EM roots was markedly reduced by a specific inhibitor of PM H^+-ATPase (sodium orthovanadate) in the presence and absence of Cd^{2+} stress (**Figure 11A**, Supplementary Figure S9) supports that the vigorous H^+ efflux is the consequence of H^+-ATPase activity. Accordingly, the increased H^+ efflux upon Cd^{2+} shock (NM, MAJ and NAU roots; **Figure 1C**), ST (MAJ and NAU roots; **Figure 5**) and LT (NM roots; **Figure 5**) stress indicates the activated H^+-pumping activity. In NM and EM roots, Cd^{2+} exposure led to a marked upregulation of *HA2.1* and *AHA10.1*, two important genes encoding PM H^+-ATPases (Ma Y. et al., 2014). The activation of PM H^+-ATPase by Cd^{2+} is likely associated with the Cd^{2+}-elicited H_2O_2, since (i) H_2O_2 increased H^+ pumping activity in *P. euphratica* callus cells (Sun et al., 2010), in roots of *P. euphratica* (Sun et al., 2010) and secretor and non-secretor mangrove species (Lu et al., 2013; Lang et al., 2014), and (ii) the expression of genes encoding PM H^+-ATPase are stimulated by H_2O_2 in *Cucumis sativus* roots (Janicka-Russak and Kabala, 2012; Janicka-Russak et al., 2012).

The activated PM H^+-ATPase enabled NM and EM roots to maintain an acidic environment, which favors the entry of Cd^{2+} across the PM (**Figure 10A**). Similarly, He et al. (2015) showed that pH 5.5 accelerates Cd^{2+} influx into poplar roots compared to pH 4.0 or pH 7.0. Moreover, the Cd^{2+} influx was markedly suppressed by the application of sodium vanadate, an

inhibitor of PM H$^+$-ATPase (**Figure 11B**). These results indicate that the PM H$^+$-pumps play a crucial role in enhancing the entry of Cd^{2+} (Ma Y. et al., 2014). Accordingly, NMT profiles of NM and EM roots showed that the maximum influx of Ca^{2+} was observed at pH 5.2 (**Figure 10B**), and that Ca^{2+} influx was blocked by sodium vanadate (**Figure 11C**). Therefore, we infer that Cd^{2+} activated H$^+$-pumping in the PM, which led to hyperpolarization of the PM and increased Cd^{2+} influx through hyperpolarization-activated Ca^{2+} channels (HACCs). However, at present we cannot exclude the possibility that Cd^{2+} ions also penetrated through depolarization-activated (DACCs) and voltage-independent Ca^{2+} channels (VICCs), because the inhibitor of PM H$^+$-ATPase, sodium vanadate, could not fully block the Cd^{2+} influx in NM and EM roots (**Figure 11B**). It has been shown that NSCCs co-exist with HACCs in the root cell plasma membrane to mediate the entry of Ca^{2+}, but the two Ca^{2+} influx routes differ in their voltage sensitivity (Demidchik et al., 2002).

Ectomycorrhizal *Populus* × *canescens* show highly activated H$^+$-pumping activity in the PM, which favors the Cd^{2+} influx through HACCs. Our NMT data showed that colonization of *P.* × *canescens* with *P. involutus* caused a marked H$^+$ efflux (**Figures 1C**, **5**, and **11A**), suggesting that the fungal colonization could activate the PM H$^+$-ATPase in ectomycorrhizas. This is consistent to our previous studies (Li J. et al., 2012; Ma X. et al., 2014). It has been documented that some host PM H$^+$-ATPase isoforms show high activity in arbuscular mycorrhizal associations (Ramos et al., 2005; Rosewarne et al., 2007). Obviously, H$^+$-pumping activity was activated by Cd^{2+}

shock and ST exposure, as the H$^+$ efflux in MAJ- and NAU-ectomycorrhizal roots were significantly higher than the NM roots (**Figures 1C** and **5**). Increased abundance of *HA2.1* and *AHA10.1* encoding PM H$^+$-ATPase in ectomycorrhizas compared to NM roots of *P.* × *canescens* were suggested to lead to higher activities of PM H$^+$-ATPases (Ma Y. et al., 2014). The highly activated PM H$^+$-ATPase, on the one hand maintains a more suitable acidic environment to promote the Cd^{2+} and Ca^{2+} influx across the PM (**Figure 10**) and on the other hand, provides an electrochemical H$^+$ gradient for PM hyperpolarization, thus increasing Cd^{2+} influx via HACCs. Accordingly, the Cd^{2+}-stimulated Cd^{2+} and Ca^{2+} in the *P. involutus* mycelia (**Figures 1–3**) was associated with the activated H$^+$ pumps since Cd^{2+} treatment markedly upregulated the transcription of PM H$^+$-ATPase 1 (Jacob et al., 2004).

Importantly, the H$_2$O$_2$ produced in the ectomycorrhizal associations may accelerate the Cd^{2+} through the PM H$^+$-ATPase-mediated HACCs. Whole-cell patch clamp recordings of *Arabidopsis* guard cells showed that the PM hyperpolarization only activates Ca^{2+} currents in the presence of H$_2$O$_2$ (50 μM to 5 mM), and the Ca^{2+} current amplitudes increase with increasing H$_2$O$_2$ concentrations (Pei et al., 2000). Demidchik et al. (2007) showed that application of H$_2$O$_2$ (10 mM) to the external PM face of elongation zone epidermal protoplasts resulted in the appearance of a hyperpolarization-activated Ca^{2+} permeable conductance. In mature epidermal protoplasts, PM HACCs were activated only when H$_2$O$_2$ was present at the intracellular membrane face, and channel opening probability increased with intracellular H$_2$O$_2$ concentrations at hyperpolarized voltages
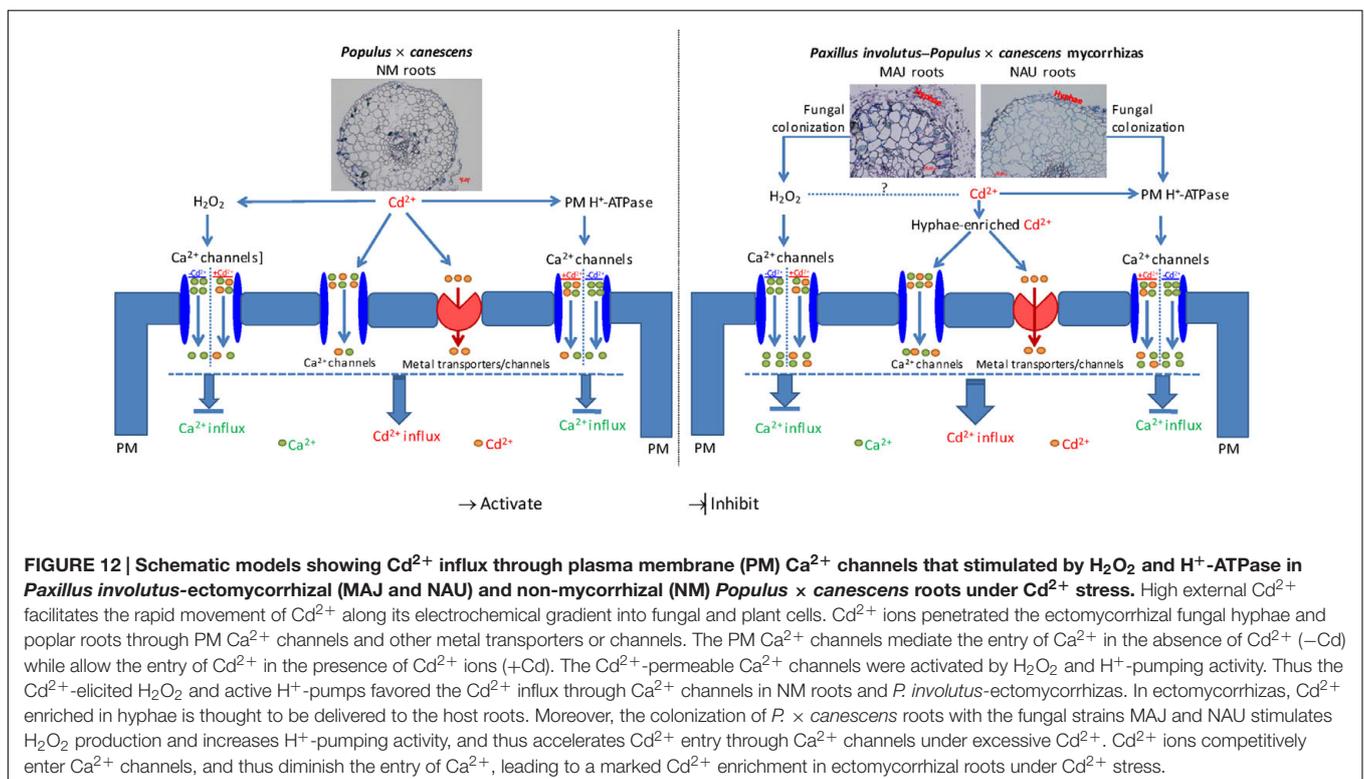
FIGURE 12 | Schematic models showing Cd^{2+} influx through plasma membrane (PM) Ca^{2+} channels that stimulated by H$_2$O$_2$ and H$^+$-ATPase in *Paxillus involutus*-ectomycorrhizal (MAJ and NAU) and non-mycorrhizal (NM) *Populus* × *canescens* roots under Cd^{2+} stress. High external Cd^{2+} facilitates the rapid movement of Cd^{2+} along its electrochemical gradient into fungal and plant cells. Cd^{2+} ions penetrated the ectomycorrhizal fungal hyphae and poplar roots through PM Ca^{2+} channels and other metal transporters or channels. The PM Ca^{2+} channels mediate the entry of Ca^{2+} in the absence of Cd^{2+} (−Cd) while allow the entry of Cd^{2+} in the presence of Cd^{2+} ions (+Cd). The Cd^{2+}-permeable Ca^{2+} channels were activated by H$_2$O$_2$ and H$^+$-pumping activity. Thus the Cd^{2+}-elicited H$_2$O$_2$ and active H$^+$-pumps favored the Cd^{2+} influx through Ca^{2+} channels in NM roots and *P. involutus*-ectomycorrhizas. In ectomycorrhizas, Cd^{2+} enriched in hyphae is thought to be delivered to the host roots. Moreover, the colonization of *P.* × *canescens* roots with the fungal strains MAJ and NAU stimulates H$_2$O$_2$ production and increases H$^+$-pumping activity, and thus accelerates Cd^{2+} entry through Ca^{2+} channels under excessive Cd^{2+}. Cd^{2+} ions competitively enter Ca^{2+} channels, and thus diminish the entry of Ca^{2+}, leading to a marked Cd^{2+} enrichment in ectomycorrhizal roots under Cd^{2+} stress.

(Demidchik et al., 2007). A massive presence of H_2O_2 was demonstrated in the outer hyphae mantle of *P. involutus* symbiosis (Gafur et al., 2004; Langenfeld-Heyser et al., 2007) and obviously could be released from the hyphae into the surrounding medium (**Figure 6**). Therefore, we suppose that in ectomycorrhizal *P. × canescens*, H_2O_2 elicited by fungal colonization stimulated Cd^{2+} influx through the HACCs that had been activated by *P. involutus* colonization. In addition, we found that Cd^{2+} influx in NAU-roots was less restricted than in MAJ-roots by DMTU and sodium orthvanadate (**Figures 9B** and **11B**). The difference in the sensitivity to antagonists of H_2O_2 and PM H^+-ATPase indicates the involvement of voltage-independent Ca^{2+} channels (VICCs) in the mediation of Cd^{2+} uptake in NAU-roots, in addition to the dominant Cd^{2+} entry through HACCs.

We noticed that LT stress in hydroponic conditions caused a pronounced shift of H^+ efflux toward an influx in EM roots (**Figure 5**). LT-stressed *P. involutus* mycelia exhibited a trend similar to that in EM roots (**Figure 5**). These results imply that ectomycorrhization activated an H^+/Cd^{2+} antiport to reduce excessive Cd^{2+} uptake and accumulation under prolonged stress conditions (Sun et al., 2013b). Similarly, we have previously shown that NaCl-treated *P. euphratica* roots retain an active PM Na^+/H^+ antiport to avoid the excessive buildup of Na^+ when exposed to LT salinity (Sun et al., 2009a,b). Here, the rate of H^+/Cd^{2+} antiport could not be determined, because our NMT data only show the net flux of the target element across the PM, instead of an unidirectional flux. In addition, EM roots were able to avoid the ROS burst in Cd^{2+} environments (**Figure 6**), probably because these roots were characterized by elevated H_2O_2 production (Gafur et al., 2004). Therefore, EM roots are likely to control the Cd^{2+} influx through the H_2O_2-activated PM Ca^{2+} channels, thus avoiding an excessive accumulation of the heavy metal ions under prolonged period of Cd^{2+} stress.

CONCLUSION

High external Cd^{2+} facilitates the rapid movement of Cd^{2+} along its electrochemical gradient into fungal and plant cells. Based on pharmacological evidence, we conclude that Cd^{2+} ions mainly penetrated the ectomycorrhizal fungal hyphae and poplar roots through PM Ca^{2+} channels. Because the entry of Cd^{2+} could not be fully blocked by various Ca^{2+} channel inhibitors ($LaCl_3$, $GdCl_3$, verapamil, and TEA), our results indicate that Cd^{2+} ions also entered the root and fungal cells through other metal transporters or channels. Our flux measurements show that the Cd^{2+}-permeable Ca^{2+} channels were activated by H_2O_2 and H^+-pumping activity. Altogether based on the current and literature data, we propose a signaling pathway that triggers Ca^{2+}-channel-mediated Cd^{2+} influx in NM *P. × canescens* roots and explains the pronounced Cd^{2+} stimulation in ectomycorrhizal associations under Cd^{2+} stress. As shown in **Figure 12**, the Cd^{2+}-elicited H_2O_2 and active H^+-pumps favored the Cd^{2+} influx through Ca^{2+} channels

in NM roots and *P. involutus*-ectomycorrhiza, while these channels mediate Ca^{2+} influx in the absence of Cd^{2+} stress. In ectomycorrhizas, Cd^{2+} enriched in hyphae is thought to be delivered to the host roots. Moreover, the colonization of *P. × canescens* roots with the fungal strains MAJ and NAU stimulates H_2O_2 production and increases H^+-pumping activity, and thus accelerates Cd^{2+} entry through Ca^{2+} channels, in particular through HACCs, under excessive Cd^{2+}. Cd^{2+} ions competitively enter Ca^{2+} channels, and thus diminish the entry of Ca^{2+}, leading to a marked Cd^{2+} enrichment in ectomycorrhizal roots under Cd^{2+} stress.

AUTHOR CONTRIBUTIONS

FUNDING

ACKNOWLEDGMENTS

SUPPLEMENTARY MATERIAL

The Supplementary Material for this article can be found online at: http://journal.frontiersin.org/article/10.3389/fpls.2016.01975/full#supplementary-material

REFERENCES

Anjum, S. A., Tanveer, M., Hussain, S., Bao, M., Wang, L., Khan, I., et al. (2015). Cadmium toxicity in Maize (*Zea mays* L.): consequences on antioxidative systems, reactive oxygen species and cadmium accumulation. *Environ. Sci. Pollut. Res.* 22, 17022–17030. doi: 10.1007/s11356-015-4882-z

Baliardini, C., Meyer, C. L., Salis, P., Saumitou-Laprade, P., and Verbruggen, N. (2015). *CATION EXCHANGER1* cosegregates with cadmium tolerance in the metal hyperaccumulator *Arabidopsis halleri* and plays a role in limiting oxidative stress in *Arabidopsis* Spp. *Plant Physiol.* 169, 549–559. doi: 10.1104/pp.15.01037

Baum, C., Hrynkiewicz, K., Leinweber, P., and Meißner, R. (2006). Heavy-metal mobilization and uptake by mycorrhizal and nonmycorrhizal willows (*Salix × dasyclados*). *J. Plant. Nutr. Soil Sci.* 169, 516–522. doi: 10.1002/jpln.200521925

Beritognolo, I., Piazzai, M., Benucci, S., Kuzminsky, E., Sabatti, M., Mugnozza, G. S., et al. (2007). Functional characterisation of three Italian *Populus alba* L. genotypes under salinity stress. *Trees* 21, 465–477. doi: 10.1007/s00468-007-0139-x

Blaudez, D., Botton, B., and Chalot, M. (2000). Cadmium uptake and subcellular compartmentation in the ectomycorrhizal fungus *Paxillus involutus*. *Microbiology* 146, 1109–1117. doi: 10.1099/00221287-146-5-1109

Blumwald, E., Aharon, G. S., and Apse, M. P. (2000). Sodium transport in plant cells. *Biochim. Biophys. Acta* 1465, 140–151. doi: 10.1016/S0005-2736(00)00135-8

Chen, L., Hu, X., Yang, W., Xu, Z., Zhang, D., and Gao, S. (2015). The effects of arbuscular mycorrhizal fungi on sex-specific responses to Pb pollution in *Populus cathayana*. *Ecotoxicol. Environ. Saf.* 113, 460–468. doi: 10.1016/j.ecoenv.2014.12.033

Chen, S., Hawighorst, P., Sun, J., and Polle, A. (2014). Salt tolerance in *Populus*: significance of stress signaling networks, mycorrhization, and soil amendments for cellular and whole-plant nutrition. *Environ. Exp. Bot.* 107, 113–124. doi: 10.1016/j.envexpbot.2014.06.001

Chen, S., and Polle, A. (2010). Salinity tolerance of *Populus*. *Plant Biol.* 12, 317–333. doi: 10.1111/j.1438-8677.2009.00301.x

Chung, J. S., Zhu, J. K., Bressan, R. A., Hasegawa, P. M., and Shi, H. (2008). Reactive oxygen species mediate Na$^+$-induced *SOS1* mRNA stability in Arabidopsis. *Plant J.* 53, 554–565. doi: 10.1111/j.1365-313X.2007.03364.x

Clemens, S. (2006). Toxic metal accumulation, responses to exposure and mechanisms of tolerance in plants. *Biochimie* 88, 1707–1719. doi: 10.1016/j.biochi.2006.07.003

Clemens, S., Antosiewicz, D. M., Ward, J. M., Schachtman, D. P., and Schroeder, J. I. (1998). The plant cDNA *LCT1* mediates the uptake of calcium and cadmium in yeast. *Proc. Natl. Acad. Sci. U.S.A.* 95, 12043–12048. doi: 10.1073/pnas.95.20.12043

Cohen, C. K., Fox, T. C., Garvin, D. F., and Kochian, L. V. (1998). The role of iron-deficiency stress responses in stimulating heavy-metal transport in plants. *Plant Physiol.* 116, 1063–1072. doi: 10.1104/pp.116.3.1063

Cosgrove, D. J., and Hedrich, R. (1991). Stretch-activated chloride, potassium, and calcium channels coexisting in plasma membranes of guard cells of *Vicia faba* L. *Planta* 186, 143–153. doi: 10.1007/BF00201510

Cosio, C., Martinoia, E., and Keller, C. (2004). Hyperaccumulation of cadmium and zinc in *Thlaspi caerulescens* and *Arabidopsis halleri* at the leaf cellular level. *Plant Physiol.* 134, 716–725. doi: 10.1104/pp.103.031948

Courbot, M., Diez, L., Ruotolo, R., Chalot, M., and Leroy, P. (2004). Cadmium-responsive thiols in the ectomycorrhizal fungus *Paxillus involutus*. *Appl. Environ. Microb.* 70, 7413–7417. doi: 10.1128/AEM.70.12.7413-7417.2004

DalCorso, G., Farinati, S., Maistri, S., and Furini, A. (2008). How plants cope with cadmium: staking all on metabolism and gene expression. *J. Integr. Plant Biol.* 50, 1268–1280. doi: 10.1111/j.1744-7909.2008.00737.x

Danielsen, L., Lohaus, G., Sirrenberg, A., Karlovsky, P., Bastien, C., Pilate, G., et al. (2013). Ectomycorrhizal colonization and diversity in relation to tree biomass and nutrition in a plantation of transgenic poplars with modified lignin biosynthesis. *PLoS ONE* 8:e59207. doi: 10.1371/journal.pone.0059207

Danielsen, L., Thürmer, A., Meinicke, P., Buee, M., Morin, E., Martin, F., et al. (2012). Fungal soil communities in a young transgenic poplar plantation form a rich reservoir for fungal root communities. *Ecol. Evol.* 2, 1935–1948. doi: 10.1002/ece3.305

Demidchik, V., Bowen, H. C., Maathuis, F. J., Shabala, S. N., Tester, M. A., White, P. J., et al. (2002). *Arabidopsis thaliana* root non-selective cation channels mediate calcium uptake and are involved in growth. *Plant J.* 32, 799–808. doi: 10.1046/j.1365-313X.2002.01467.x

Demidchik, V., Shabala, S. N., and Davies, J. M. (2007). Spatial variation in H$_2$O$_2$ response of *Arabidopsis thaliana* root epidermal Ca^{2+} flux and plasma membrane Ca^{2+} channels. *Plant J.* 49, 377–386. doi: 10.1111/j.1365-313X.2006.02971.x

Demidchik, V., Shang, Z., Shin, R., Thompson, E., Rubio, L., Laohavisit, A., et al. (2009). Plant extracellular ATP signalling by plasma membrane NADPH oxidase and Ca^{2+} channels. *Plant J.* 58, 903–913. doi: 10.1111/j.1365-313X.2009.03830.x

Duplessis, S., Courty, P. E., Tagu, D., and Martin, F. (2005). Transcript patterns associated with ectomycorrhiza development in *Eucalyptus globulus* and *Pisolithus microcarpus*. *New Phytol.* 165, 599–611. doi: 10.1111/j.1469-8137.2004.01248.x

Gafur, A., Schützendübel, A., Langenfeld-Heyser, R., Fritz, E., and Polle, A. (2004). Compatible and incompetent *Paxillus involutus* isolates for ectomycorrhiza formation *in vitro* with poplar (*Populus × canescens*) differ in H$_2$O$_2$ production. *Plant Biol.* 6, 91–99. doi: 10.1055/s-2003-44718

Gallego, S. M., Pena, L. B., Barcia, R. A., Azpilicueta, C. E., Iannone, M. F., Rosales, E. P., et al. (2012). Unravelling cadmium toxicity and tolerance in plants: insight into regulatory mechanisms. *Environ. Exp. Bot.* 83, 33–46. doi: 10.1016/j.envexpbot.2012.04.006

Garg, N., and Aggarwal, N. (2012). Effect of mycorrhizal inoculations on heavy metal uptake and stress alleviation of *Cajanus cajan* (L.) Millsp. genotypes grown in cadmium and lead contaminated soils. *Plant Growth Regul.* 66, 9–26. doi: 10.1007/s10725-011-9624-8

Gelli, A., and Blumwald, E. (1997). Hyperpolarization-activated Ca^{2+}-permeable channels in the plasma membrane of tomato cells. *J. Membr. Biol.* 155, 35–45. doi: 10.1007/s002329900156

Grabov, A., and Blatt, M. R. (1998). Membrane voltage initiates Ca^{2+} waves and potentiates Ca^{2+} increases with abscisic acid in stomatal guard cells. *Proc. Natl. Acad. Sci. U.S.A.* 95, 4778–4783. doi: 10.1007/s002329900156

Grabov, A., and Blatt, M. R. (1999). A steep dependence of inward-rectifying potassium channels on cytosolic free calcium concentration increase evoked by hyperpolarization in guard cells. *Plant Physiol.* 119, 277–288. doi: 10.1104/pp.119.1.277

Gussarsson, M., Asp, H., Adalsteinsson, S., and Jensén, P. (1996). Enhancement of cadmium effects on growth and nutrient composition of birch (*Betula pendula*) by buthionine sulphoximine (BSO). *J. Exp. Bot.* 47, 211–215. doi: 10.1093/jxb/47.2.211

Han, Y., Sa, G., Sun, J., Shen, Z., Zhao, R., Ding, M., et al. (2014). Overexpression of *Populus euphratica* xyloglucan endotransglucosylase/hydrolase gene confers enhanced cadmium tolerance by the restriction of root cadmium uptake in transgenic tobacco. *Environ. Exp. Bot.* 100, 74–83. doi: 10.1016/j.envexpbot.2013.12.021

Han, Y., Wang, S., Zhao, N., Deng, S., Zhao, C., Li, N., et al. (2016). Exogenous abscisic acid alleviates cadmium toxicity by restricting Cd^{2+} influx in *Populus euphratica* cells. *J. Plant Growth Regul.* 35, 827–837. doi: 10.1007/s00344-016-9585-2

He, J., Li, H., Luo, J., Ma, C., Li, S., Qu, L., et al. (2013). A transcriptomic network underlies microstructural and physiological responses to cadmium in *Populus × canescens*. *Plant Physiol.* 162, 424–439. doi: 10.1104/pp.113.215681

He, J., Li, H., Ma, C., Zhang, Y., Polle, A., Rennenberg, H., et al. (2015). Overexpression of bacterial γ-glutamylcysteine synthetase mediates changes in cadmium influx, allocation and detoxification in poplar. *New Phytol.* 205, 240–254. doi: 10.1111/nph.13013

He, J., Qin, J., Long, L., Ma, Y., Li, H., Li, K., et al. (2011). Net cadmium flux and accumulation reveal tissue-specific oxidative stress and detoxification in *Populus × canescens*. *Physiol. Plant.* 143, 50–63. doi: 10.1111/j.1399-3054.2011.01487.x

Hirschi, K. D., Korenkov, V. D., Wilganowski, N. L., and Wagner, G. J. (2000). Expression of Arabidopsis *CAX2* in tobacco. Altered metal accumulation and increased manganese tolerance. *Plant Physiol.* 124, 125–134. doi: 10.1104/pp.124.1.125

Jacob, C., Courbot, M., Brun, A., Steinman, H. M., Jacquot, J. P., Botton, B., et al. (2001). Molecular cloning, characterization and regulation by cadmium of a

superoxide dismutase from the ectomycorrhizal fungus *Paxillus involutus*. *Eur. J. Biochem.* 268, 3223–3232. doi: 10.1046/j.1432-1327.2001.02216.x

Jacob, C., Courbot, M., Martin, F., Brun, A., and Chalot, M. (2004). Transcriptomic responses to cadmium in the ectomycorrhizal fungus *Paxillus involutus*. *FEBS Lett.* 576, 423–427. doi: 10.1016/j.febslet.2004.09.028

Janicka-Russak, M., and Kabala, K. (2012). Abscisic acid and hydrogen peroxide induce modification of plasma membrane H^+-ATPase from *Cucumis sativus* L. roots under heat shock. *J. Plant Physiol.* 169, 1607–1614. doi: 10.1016/j.jplph.2012.05.013

Janicka-Russak, M., Kabala, K., Wdowikowska, A., and Klobus, G. (2012). Response of plasma membrane H^+-ATPase to low temperature in cucumber roots. *J. Plant Res.* 125, 291–300. doi: 10.1007/s10265-011-0438-6

Kaplan, O., Ince, M., and Yaman, M. (2011). Sequential extraction of cadmium in different soil phases and plant parts from a former industrialized area. *Environ. Chem. Lett.* 9, 397–404. doi: 10.1007/s10311-010-0292-0

Kieffer, P., Schröder, P., Dommes, J., Hoffmann, L., Renaut, J., and Hausman, J. F. (2009). Proteomic and enzymatic response of poplar to cadmium stress. *J. Proteomics* 72, 379–396. doi: 10.1016/j.jprot.2009.01.014

Kim, D. Y., Bovet, L., Kushnir, S., Noh, E. W., Martinoia, E., and Lee, Y. (2006). AtATM3 is involved in heavy metal resistance in Arabidopsis. *Plant Physiol.* 140, 922–932. doi: 10.1104/pp.105.074146

Krämer, U. (2010). Metal hyperaccumulation in plants. *Annu. Rev. Plant Biol.* 61, 517–534. doi: 10.1146/annurev-arplant-042809-112156

Krpata, D., Fitz, W., Peintner, U., Langer, I., and Schweiger, P. (2009). Bioconcentration of zinc and cadmium in ectomycorrhizal fungi and associated aspen trees as affected by level of pollution. *Environ. Pollut.* 157, 280–286. doi: 10.1016/j.envpol.2008.06.038

Krpata, D., Peintner, U., Langer, I., Fitz, W. J., and Schweiger, P. (2008). Ectomycorrhizal communities associated with *Populus tremula* growing on a heavy metal contaminated site. *Mycol. Res.* 112, 1069–1079. doi: 10.1016/j.mycres.2008.02.004

Lang, T., Sun, H., Li, N., Lu, Y., Shen, Z., Jing, X., et al. (2014). Multiple signaling networks of extracellular ATP, hydrogen peroxide, calcium, and nitric oxide in the mediation of root ion fluxes in secretor and non-secretor mangroves under salt stress. *Aquat. Bot.* 119, 33–43. doi: 10.1016/j.aquabot.2014.06.009

Langenfeld-Heyser, R., Gao, J., Ducic, T., Tachd, P., Lu, C. F., Fritz, E., et al. (2007). *Paxillus involutus* mycorrhiza attenuate NaCl-stress responses in the salt-sensitive hybrid poplar *Populus × canescens*. *Mycorrhiza* 17, 121–131. doi: 10.1007/s00572-006-0084-3

Leple, J. C., Brasileiro, A. C. M., Michel, M. F., Delmotte, F., and Jouanin, L. (1992). Transgenic poplars: expression of chimeric genes using four different constructs. *Plant Cell Rep.* 11, 137–141. doi: 10.1007/BF00232166

Li, J., Bao, S., Zhang, Y., Ma, X., Mishra-Knyrim, M., Sun, J., et al. (2012). *Paxillus involutus* strains MAJ and NAU mediate K^+/Na^+ homeostasis in ectomycorrhizal *Populus × canescens* under sodium chloride stress. *Plant Physiol.* 159, 1771–1786. doi: 10.1104/pp.112.195370

Li, L., Liu, X., Peijnenburg, W. J., Zhao, J., Chen, X., Yu, J., et al. (2012a). Pathways of cadmium fluxes in the root of the halophyte *Suaeda salsa*. *Ecotoxicol. Environ. Saf.* 75, 1–7. doi: 10.1016/j.ecoenv.2011.09.007

Li, L., Liu, X., You, L., Zhang, L., Zhao, J., and Wu, H. (2012b). Uptake pathways and subcellular fractionation of Cd in the polychaete *Nereis diversicolor*. *Ecotoxicology* 21, 104–110. doi: 10.1007/s10646-011-0770-6

Lin, Y. F., and Aarts, M. G. (2012). The molecular mechanism of zinc and cadmium stress response in plants. *Cell Mol. Life. Sci.* 69, 3187–3206. doi: 10.1007/s00018-012-1089-z

Liu, X. F., Supek, F., Nelson, N., and Culotta, V. C. (1997). Negative control of heavy metal uptake by the *Saccharomyces cerevisiae* BSD2 gene. *J. Biol. Chem.* 272, 11763–11769. doi: 10.1074/jbc.272.18.11763

Lu, L., Tian, S., Zhang, M., Zhang, J., Yang, X., and Jiang, H. (2010). The role of Ca pathway in Cd uptake and translocation by the hyperaccumulator *Sedum alfredii*. *J. Hazard. Mater.* 183, 22–28. doi: 10.1016/j.jhazmat.2010.06.036

Lu, Y., Li, N., Sun, J., Hou, P., Jing, X., Zhu, H., et al. (2013). Exogenous hydrogen peroxide, nitric oxide and calcium mediate root ion fluxes in two non-secretor mangrove species subjected to NaCl stress. *Tree Physiol.* 33, 81–95. doi: 10.1093/treephys/tps119

Luo, J., Qin, J., He, F., Li, H., Liu, T., Polle, A., et al. (2013). Net fluxes of ammonium and nitrate in association with H^+ fluxes in fine roots of *Populus populari*s. *Planta* 237, 919–931. doi: 10.1007/s00425-012-1807-7

Luo, Z. B., Janz, D., Jiang, X., Göbel, C., Wildhagen, H., Tan, Y., et al. (2009). Upgrading root physiology for stress tolerance by ectomycorrhizas: insights from metabolite and transcriptional profiling into reprogramming for stress anticipation. *Plant Physiol.* 151, 1902–1917. doi: 10.1104/pp.109.143735

Luo, Z. B., Li, K., Gai, Y., Göbel, C., Wildhagen, H., Jiang, X., et al. (2011). The ectomycorrhizal fungus (*Paxillus involutus*) modulates leaf physiology of poplar towards improved salt tolerance. *Environ. Exp. Bot.* 72, 304–311. doi: 10.1016/j.envexpbot.2011.04.008

Luo, Z. B., Wu, C., Zhang, C., Li, H., Lipka, U., and Polle, A. (2014). The role of ectomycorrhizas in heavy metal stress tolerance of host plants. *Environ. Exp. Bot.* 108, 47–62. doi: 10.1016/j.envexpbot.2013.10.018

Ma, X., Deng, L., Li, J., Zhou, X., Li, N., Zhang, D., et al. (2010). Effect of NaCl on leaf H^+-ATPase and the relevance to salt tolerance in two contrasting poplar species. *Trees* 24, 597–607. doi: 10.1007/s00468-010-0430-0

Ma, X., Sun, M., Sa, G., Zhang, Y., Li, J., Sun, J., et al. (2014). Ion fluxes in *Paxillus involutus*-inoculated roots of *Populus × canescens* under saline stress. *Environ. Exp. Bot.* 108, 99–108. doi: 10.1016/j.envexpbot.2013.11.016

Ma, Y., He, J., Ma, C., Luo, J., Li, H., Liu, T., et al. (2014). Ectomycorrhizas with *Paxillus involutus* enhance cadmium uptake and tolerance in *Populus × canescens*. *Plant Cell Environ.* 37, 627–642. doi: 10.1111/pce.12183

Mendoza-Cózatl, D. G., Jobe, T. O., Hauser, F., and Schroeder, J. I. (2011). Long-distance transport, vacuolar sequestration, tolerance, and transcriptional responses induced by cadmium and arsenic. *Curr. Opin. Plant Biol.* 14, 554–562. doi: 10.1016/j.pbi.2011.07.004

Migeon, A., Blaudez, D., Wilkins, O., Montanini, B., Campbell, M. M., Richaud, P., et al. (2010). Genome-wide analysis of plant metal transporters, with an emphasis on poplar. *Cell. Mol. Life Sci.* 67, 3763–3784. doi: 10.1007/s00018-010-0445-0

Milner, M. J., and Kochian, L. V. (2008). Investigating heavy-metal hyperaccumulation using *Thlaspi caerulescens* as a model system. *Ann. Bot* 102, 3–13. doi: 10.1093/aob/mcn063

Murashige, T., and Skoog, F. (1962). A revised medium for rapid growth and bio assays with tobacco tissue cultures. *Physiol. Plant.* 15, 473–497. doi: 10.1111/j.1399-3054.1962.tb08052.x

Nawrot, T., Plusquin, M., Hogervorst, J., Roels, H. A., Celis, H., Thijs, L., et al. (2006). Environmental exposure to cadmium and risk of cancer: a prospective population-based study. *Lancet Oncol.* 7, 119–126. doi: 10.1016/S1470-2045(06)70545-9

Ott, T., Fritz, E., Polle, A., and Schützendübel, A. (2002). Characterisation of antioxidative systems in the ectomycorrhiza-building basidiomycete *Paxillus involutus* (Bartsch) Fr. and its reaction to cadmium. *FEMS Microbiol. Ecol.* 42, 359–366. doi: 10.1111/j.1574-6941.2002.tb01025.x

Papoyan, A., Piñeros, M., and Kochian, L. V. (2007). Plant Cd^{2+} and Zn^{2+} status effects on root and shoot heavy metal accumulation in *Thlaspi caerulescens*. *New Phytol.* 175, 51–58. doi: 10.1111/j.1469-8137.2007.02073.x

Pei, Z. M., Murata, Y., Benning, G., Thomine, S., Klüsener, B., Allen, G. J., et al. (2000). Calcium channels activated by hydrogen peroxide mediate abscisic acid signalling in guard cells. *Nature* 406, 731–734. doi: 10.1038/35021067

Perfus-Barbeoch, L., Leonhardt, N., Vavasseur, A., and Forestier, C. (2002). Heavy metal toxicity: cadmium permeates through calcium channels and disturbs the plant water status. *Plant J.* 32, 539–548. doi: 10.1046/j.1365-313X.2002.01442.x

Pickard, B. G., and Ding, J. P. (1993). The mechanosensory calcium-selective ion channel: key component of a plasmalemmal control centre? *Aust. J. Plant Physiol.* 20, 439–459. doi: 10.1071/PP9930439

Piñeros, M., and Tester, M. (1997). Calcium channels in higher plant cells: selectivity, regulation and pharmacology. *J. Exp. Bot.* 48, 551–577. doi: 10.1093/jxb/48

Ping, Z., Yabe, I., and Muto, S. (1992). Voltage-dependent Ca^{2+} channels in the plasma membrane and the vacuolar membrane of *Arabidopsis thaliana*. *Biochim. Biophys Acta* 1112, 287–290. doi: 10.1016/0005-2736(92)90404-A

Piqueras, A., Olmos, E., Martinez-Solano, J. R., and Hellin, E. (1999). Cd-induced oxidative burst in tobacco BY2 cells: time course, subcellular location and antioxidant response. *Free Radic. Res.* 31, S33–S38. doi: 10.1080/10715769900301291

Plaza, S., Tearall, K. L., Zhao, F. J., Buchner, P., McGrath, S. P., and Hawkesford, M. J. (2007). Expression and functional analysis of metal transporter genes in two contrasting ecotypes of the hyperaccumulator *Thlaspi caerulescens*. *J. Exp. Bot.* 58, 1717–1728. doi: 10.1093/jxb/erm025

Polle, A., and Chen, S. (2015). On the salty side of life: molecular, physiological and anatomical adaptation and acclimation of trees to extreme habitats. *Plant Cell Environ.* 38, 1794–1816. doi: 10.1111/pce.12440

Polle, A., Klein, T., and Kettner, C. (2013). Impact of cadmium on young plants of *Populus euphratica* and *P. × canescens*, two poplar species that differ in stress tolerance. *New For.* 44, 13–22. doi: 10.1007/s11056-011-9301-9

Ramos, A. C., Martins, M. A., and Façanha, A. R. (2005). ATPase and pyrophosphatase activities in corn root microsomes colonized with arbuscular mycorrhizal fungi. *Braz. J. Plant Physiol.* 29, 207–213. doi: 10.1590/S0100-06832005000200006

Rodríguez-Serrano, M., Romero-Puertas, M. C., Pazmiño, D. M., Testillano, P. S., Risueno, M. C., Río, L. A., et al. (2009). Cellular response of pea plants to cadmium toxicity: cross talk between reactive oxygen species, nitric oxide, and calcium. *Plant Physiol.* 150, 229–243. doi: 10.1104/pp.108.131524

Rosewarne, G. M., Smith, F. A., Schachtman, D. P., and Smith, S. E. (2007). Localization of proton-ATPase genes expressed in arbuscular mycorrhizal tomato plants. *Mycorrhiza* 17, 249–258. doi: 10.1007/s00572-006-0101-6

Roth, U., von Roepenack-Lahaye, E., and Clemens, S. (2006). Proteome changes in *Arabidopsis thaliana* roots upon exposure to Cd^{2+}. *J. Exp. Bot.* 57, 4003–4013. doi: 10.1093/jxb/erl170

Rozpądek, P., Węzowicz, K., Stojakowska, A., Malarz, J., Surówka, E., Sobczyk, L., et al. (2014). Mycorrhizal fungi modulate phytochemical production and antioxidant activity of *Cichorium intybus* L. (*Asteraceae*) under metal toxicity. *Chemosphere* 112, 217–224. doi: 10.1016/j.chemosphere.2014.04.023

Salzer, P., Corbière, H., and Boller, T. (1999). Hydrogen peroxide accumulation in *Medicago truncatula* roots colonized by the arbuscular mycorrhiza-forming fungus *Glomus intraradices*. *Planta* 208, 319–325. doi: 10.1007/s004250050565

Schützendübel, A., Nikolova, P., Rudolf, C., and Polle, A. (2002). Cadmium and H_2O_2-induced oxidative stress in *Populus × canescens* roots. *Plant Physiol. Biochem.* 40, 577–584. doi: 10.1016/S0981-9428(02)01411-0

Schützendübel, A., and Polle, A. (2002). Plant responses to abiotic stresses: heavy metal-induced oxidative stress and protection by mycorrhization. *J. Exp. Bot.* 53, 1351–1365. doi: 10.1093/jexbot/53.372.1351

Schützendübel, A., Schwanz, P., Teichmann, T., Gross, K., Langenfeld-Heyser, R., Godbold, D. L., et al. (2001). Cadmium-induced changes in antioxidative systems, hydrogen peroxide content, and differentiation in scots pine roots. *Plant Physiol.* 127, 887–898. doi: 10.1104/pp.010318

Sell, J., Kayser, A., Schulin, R., and Brunner, I. (2005). Contribution of ectomycorrhizal fungi to cadmium uptake of poplars and willows from a heavily polluted soil. *Plant Soil* 277, 245–253. doi: 10.1007/s11104-005-7084-5

Shabala, S., and Knowles, A. (2002). Rhythmic patterns of nutrient acquisition by wheat roots. *Funct. Plant Biol.* 29, 595–605. doi: 10.1071/PP01130

Shabala, S., Shabala, L., Gradmann, D., Chen, Z., Newman, I., and Mancuso, S. (2006). Oscillations in plant membrane transport: model predictions, experimental validation, and physiological implications. *J. Exp. Bot.* 57, 171–184. doi: 10.1093/jxb/erj022

Shabala, S., Shabala, L., and Van Volkenburgh, E. (2003). Effect of calcium on root development and root ion fluxes in salinised barley seedlings. *Funct. Plant Biol.* 30, 507–514. doi: 10.1071/FP03016

Shabala, S. N., Newman, I. A., and Morris, J. (1997). Oscillations in H^+ and Ca^{2+} ion fluxes around the elongation region of corn roots and effects of external pH. *Plant Physiol.* 113, 111–118. doi: 10.1104/pp.113.1.111

Sousa, N. R., Ramos, M. A., Marques, A. P., and Castro, P. M. (2012). The effect of ectomycorrhizal fungi forming symbiosis with *Pinus pinaster* seedlings exposed to cadmium. *Sci. Total Environ.* 414, 63–67. doi: 10.1016/j.scitotenv.2011.10.053

Sun, J., Chen, S., Dai, S., Wang, R., Li, N., Shen, X., et al. (2009a). NaCl-induced alternations of cellular and tissue ion fluxes in roots of salt-resistant and salt-sensitive poplar species. *Plant Physiol.* 149, 1141–1153. doi: 10.1104/pp.108.129494

Sun, J., Dai, S., Wang, R., Chen, S., Li, N., Zhou, X., et al. (2009b). Calcium mediates root K^+/Na^+ homeostasis in poplar species differing in salt tolerance. *Tree Physiol.* 29, 1175–1186. doi: 10.1093/treephys/tpp048

Sun, J., Wang, M. J., Ding, M. Q., Deng, S. R., Liu, M. Q., Lu, C. F., et al. (2010). H_2O_2 and cytosolic Ca^{2+} signals triggered by the PM H^+-coupled transport system mediate K^+/Na^+ homeostasis in NaCl-stressed *Populus euphratica* cells. *Plant Cell Environ.* 33, 943–958. doi: 10.1111/j.1365-3040.2010.02118.x

Sun, J., Wang, R., Liu, Z., Ding, Y., and Li, T. (2013a). Non-invasive microelectrode cadmium flux measurements reveal the spatial characteristics and real-time kinetics of cadmium transport in hyperaccumulator and nonhyperaccumulator ecotypes of *Sedum alfredii*. *J. Plant Physiol.* 170, 355–359. doi: 10.1016/j.jplph.2012.10.014

Sun, J., Wang, R., Zhang, X., Yu, Y., Zhao, R., Li, Z., et al. (2013b). Hydrogen sulfide alleviates cadmium toxicity through regulations of cadmium transport across the plasma and vacuolar membranes in *Populus euphratica* cells. *Plant Physiol. Biochem.* 65, 67–74. doi: 10.1016/j.plaphy.2013.01.003

Sun, J., Zhang, C. L., Deng, S. R., Lu, C. F., Shen, X., Zhou, X. Y., et al. (2012). An ATP signalling pathway in plant cells: extracellular ATP triggers programmed cell death in *Populus euphratica*. *Plant Cell Environ.* 35, 893–916. doi: 10.1111/j.1365-3040.2011.02461.x

Tan, S. Y., Jiang, Q. Y., Zhuo, F., Liu, H., Wang, Y. T., Li, S. S., et al. (2015). Effect of inoculation with *Glomus versiforme* on cadmium accumulation, antioxidant activities and phytochelatins of *Solanum photeinocarpum*. *PLoS ONE* 10:e0132347. doi: 10.1371/journal.pone.0132347

Thomine, S., Wang, R., Ward, J. M., Crawford, N. M., and Schroeder, J. I. (2000). Cadmium and iron transport by members of a plant metal transporter family in *Arabidopsis* with homology to *Nramp* genes. *Proc. Natl. Acad. Sci. U.S.A.* 97, 4991–4996. doi: 10.1073/pnas.97.9.4991

Thuleau, P., Moreau, M., Schroeder, J. I., and Ranjeva, R. (1994a). Recruitment of plasma membrane voltage-dependent calcium-permeable channels in carrot cells. *EMBO J.* 13, 5843–5847.

Thuleau, P., Schroeder, J. I., and Ranjeva, R. (1998). Recent advances in the regulation of plant calcium channels: evidence for regulation by G-proteins, the cytoskeleton and second messengers. *Curr. Opin. Plant Biol* 1, 424–427. doi: 10.1016/S1369-5266(98)80267-7

Thuleau, P., Ward, J. M., Ranjeva, R., and Schroeder, J. I. (1994b). Voltage-dependent calcium-permeable channels in the plasma membrane of a higher plant cell. *EMBO J.* 13, 2970–2975.

Twig, G., Jung, S. K., Messerli, M. A., Smith, P. J., and Shirihai, O. S. (2001). Real-time detection of reactive oxygen intermediates from single microglial cells. *Biol. Bull.* 201, 261–262. doi: 10.2307/1543355

Weiss, G. B. (1974). Cellular pharmacology of lanthanum. *Annu. Rev. Pharmacol.* 14, 343–354. doi: 10.1146/annurev.pa.14.040174.002015

White, P. J. (1998). Calcium channels in the plasma membrane of root cells. *Ann. Bot.* 81, 173–183. doi: 10.1006/anbo.1997.0554

White, P. J. (2000). Calcium channels in higher plants. *Biochim. Biophys. Acta* 1465, 171–189. doi: 10.1016/S0005-2736(00)00137-1

Zhao, F. J., Hamon, R. E., Lombi, E., McLaughlin, M. J., and McGrath, S. P. (2002). Characteristics of cadmium uptake in two contrasting ecotypes of the hyperaccumulator *Thlaspi caerulescens*. *J. Exp. Bot.* 53, 535–543. doi: 10.1093/jexbot/53.368.535

Zhao, F. J., Jiang, R. F., Dunham, S. J., and McGrath, S. P. (2006). Cadmium uptake, translocation and tolerance in the hyperaccumulator *Arabidopsis halleri*. *New Phytol.* 172, 646–654. doi: 10.1111/j.1469-8137.2006.01867.x

Zhu, J. K. (2003). Regulation of ion homeostasis under salt stress. *Curr. Opin. Plant Biol.* 6, 441–445. doi: 10.1016/S1369-5266(03)00085-2

Zimmermann, S., Nürnberger, T., Frachisse, J. M., Wirtz, W., Guern, J., Hedrich, R., et al. (1997). Receptor-mediated activation of a plant Ca^{2+}-permeable ion channel involved in pathogen defense. *Proc. Natl. Acad. Sci. U.S.A.* 94, 2751–2755. doi: 10.1073/pnas.94.6.2751